Table 1. *RAF1* Mutations Identified in This Study*

Patient ID	Country of origin	Final diagnosis	Exon	Nucleotide change	Amino acid change	Domain	Genotype of father/mother
NS213	France	atypical NS	5	c. 572G>T	p.R191I[a]	CR1	NA
NS39	Japan	NS	7	c.770C>T	p.S257L	CR2	NA
NS86	France	NS	3, 7	c.309C>G	p.H103Q	CR1,	H103Q/WT
				c.770C>T	p. S257L	CR2	WT/WT
NS92	Germany	NS	7	c.770C>T	p.S257L	CR2	WT/WT
NS135	Japan	NS	7	c.770C>T	p.S257L	CR2	NA
NS146	Spain	NS	7	c.770C>T	p.S257L	CR2	NA
NS199	Japan	NS	7	c.770C>T	p.S257L	CR2	NA
NS200	France	NS	7	c.770C>T	p.S257L	CR2	NA
NS215	Japan	NS	7	c.770C>T	p.S257L	CR2	NA
NS227	Japan	NS	7	c.770C>T	p.S257L	CR2	NA
NS256	Japan	NS	7	c.770C>T	p.S257L	CR2	NA
NS258	Japan	NS	7	c.770C>T	p.S257L	CR2	WT/WT
NS279	Japan	NS	7	c.776C>T	p.S259F	CR2	NA
NS210	France	NS	7	c.781C>G	p.P261A	CR2	WT/WT
NS205	France	CS[b]	7	c.782C>T	p.P261L	CR2	NA
NS209	France	CS[c]	7	c.786T>A	p.N262K[a]	CR2	WT/WT
NS222	Japan	NS	12	c.1279A>G	p.S427G[d]	CR3	WT/p.S427G
NS285	Japan	NS	17	c.1837C>G	p.L613V	CR3	NA

NS, Noonan syndrome; CS, Costello syndrome; WT, wild type; CR, conserved region; NA, not available.
*GenBank RefSeq: NM_002880.3 Nucleotide numbering reflects cDNA numbering with +1 corresponding to the A of the ATG translation initiation codon in the reference sequence, according to journal guidelines (www.hgvs.org/mutnomen). The initiation codon is codon 1.
[a]Novel mutation.
[b]Detailed clinical manifestations were not obtained.
[c]The patient died at 1 month.
[d]The mutation was previously identified in a patient with a therapy-related acute leukemia.

ASD (31%), arrhythmia (38%), and mitral valve anomaly (29%). Other observed clinical features were hyperelastic skin (58%), curly hair (47%), and cryptorchidism in males (50%). Coagulation defects were observed in two patients.

Four patients with *RAF1* mutations died before 5 years of age (Supp. Table S2). Patient NS39 were diagnosed as having cystic hygroma in the prenatal period and had suffered from neonatal hypertrophic cardiomyopathy. At 1 year of age, she contracted acute respiratory distress syndrome after having pneumonia and died of respiratory failure. Patient NS199 had been suspected to have achondroplasia because of short limbs. He was diagnosed as having NS at 3 years of age because of distinct facial features, growth failure, short stature, and hypertrophic cardiomyopathy. He had pneumonia without fever for a week and died suddenly at 5 years of age. Patient NS227 suffered from feeding difficulties, ectopic atrial tachycardia, as well as VSD and pulmonary hypertension. The patient died at 2 months of tachycardia (>200/min) and laryngeal edema.

Clinical manifestations in our patients with *RAF1* mutations were compared with those previously reported (Table 2). The high frequency of hypertrophic cardiomyopathy in our study (63%) was consistent with that observed in patients with *RAF1* mutations previously reported (77%). The frequency of ASD and that of mitral valve anomaly were similar to those of the previous studies. However, the frequency of PS in our study (47%) was higher than that previously reported (11%). Arrhythmia was less frequently observed in our patients with *RAF1* mutations (38 vs. 89%). The frequency of mental retardation (55%) was almost same as that of the previous studies (56%). Hyperelastic skin (58%) and coagulation defects (two cases) were also described in previously reported patients with *RAF1* mutations (24% and one case, respectively).

Phosphorylation State of Mutant RAF1 Proteins

RAF1 is a ubiquitously expressed RAF serine/threonine kinase, which regulates the RAS pathway. It has been shown that phosphorylation of serine, threonine, and tyrosine residues contributes to a conformational change of RAF1 protein and activation in growth factor stimulation [Mercer and Pritchard, 2003]. In the inactive state, phosphorylated S259 and S621 serve as binding sites for 14-3-3, leading to a closed confirmation [Dhillon et al., 2007]. Phosphorylation of S621 seems essential for RAF1 activation. In contrast, phosphorylation of serine 259 has been shown to have an inhibitory role in RAF1 activation. When cells are stimulated with growth factors, dephosphorylation of S259 by protein phosphatase 1 (PP1) and/or protein phosphatase 2A (PP2A) promotes the dissociation of 14-3-3 from RAF1, resulting in an activated conformation of RAF1 protein. For full activation, multiple residues, including S338, are phosphorylated and substrate of RAF1 enters the catalytic cleft in the CR3 kinase domain. Negative feedback from activated ERK results in the phosphorylation of S289, 296, and 301 [Dhillon et al., 2007].

To examine the phosphoryalation status of mutants observed in NS patients, we transfected constructs harboring WT *RAF1* cDNA and five mutants identified in NS patients. Immunoblotting was performed using four phospho-specific antibodies of RAF1 (Fig. 2A). We first analyzed the phosphorylation status of two phosphorylation sites, S259 and S621, using antibodies that recognize each site. Immunoblotting showed that phosphorylation of S259 was scarcely observed in cell lysates expressing p.S257L and p.N262K. In contrast, phosphorylation of S259 of p.H103Q, p.R191I, and p.S427G was similar to that in WT RAF1. To confirm this observation, immunoprecipitation was performed using an anti-Myc antibody, and phosphorylation levels at S259 were examined (Fig. 2B). Immunoprecipitated RAF1 mutants (p.S257L and p.N262K) were not phosphorylated at S259, confirming that these mutants had impaired phosphorylation of S259. The phosphorylation level of S621 in four mutants (p.H103Q, p.R191I, p.S257L, and p.N262K) was similar to that in WT (Fig. 2A), whereas that in cells expressing p.S427G was enhanced. Phosphorylation levels at S338 and S289/296/301 were similar to that in WT except for p.S427G (Fig. 2A).

Phosphorylation levels at S259, S289/296/301, S338, and S621 were shown to be enhanced in cells expressing p.S427G. The expression of p.S427G appeared enhanced and the band was

Table 2. Clinical Manifestations in *RAF1*-Positive Patients in This Study and Past Studies

	Present cohort (%)	NS with *RAF1* mutations (%)	LS with *RAF1* mutations (%)
Number of patients in total	17	35[a]	2
Perinatal abnormality			
Polyhydramnios	6/15 (40)	6/19 (32)	ND
Fetal macrosomia	5/11 (45)	6/20 (30)	ND
Growth and development			
Failure to thrive in infancy	10/12(83)	3	ND
Mental retardation	6/11 (55)	19/34 (56)	1
Outcome			
Died	4/17 (24)	2/11 (18)	ND
Craniofacial characteristics			
Relative macrocephaly	16/17 (94)	16/21 (76)	ND
Hypertelorism	14/15 (93)	20/21 (95)	2
Downslanting palpebral fissures	10/16 (63)	19/21 (90)	2
Ptosis	9/16 (56)	19/21 (90)	1
Epicanthal folds	12/14 (86)	12/21 (57)	1
Low-set ears	14/15 (93)	18/21 (86)	2
Skeletal characteristics			
Short stature	11/15 (73)	30/35 (86)	2
Short neck	14/15 (93)	21/31 (68)	2
Webbing of neck	13/16 (81)	25/30 (83)	2
Cardiac defects			
Hypertrophic cardiomyopathy	10/16 (63)	27/35 (77)	2
Atrial septal defect	5/16 (31)	11/35 (31)	0
Ventricular septal defect	3/17 (18)	3/35 (9)	0
Pulmonic stenosis	7/15 (47)	4/35 (11)	1
Patent ductus arteriosus	2/17 (12)	ND	ND
Mitral valve anomaly	5/17 (29)	8/32 (25)	2
Arrhythmia	6/16 (38)	8/9 (89)	ND
Others	TR 1, PH 1, atrioventricular valve dysplasia 1, valvular AS 1	polyvalvular dysplasia 2 pulmonary valve dysplasia 1, PFO 1, TOF 2, AS 1, right shaft deflection 1	
Skeletal/extremity deformity			
Cubitus valgus	2/9 (22)	7/22 (32)	2
Pectus deformity	5/13 (38)	20/31 (65)	2
Others		prominent finger pads 2	prominent finger pads 1
Skin/hair anomaly			
Curly hair	8/17 (47)	6/24 (25)	2
Hyperelastic skin	7/12 (58)	5/21 (24)	2
Café au lait spots	1/14 (7)	2/20 (10)	2
Lentigines	1/14 (7)	2/21 (10)	2
Naevus	3/15 (20)	9/22 (41)	0
Others	low posterior implantation 4, hyperpigmentation 3, redundant skin 3, sparse hair 2, sparse eyebrows 2, hemangioma 2	dry skin 3, sparse hair 3, sparse eyebrows 2, keratosis pilaris 2	
Genitalia	6/11 (55)	11/16 (69)	
Cryptorchidism	5/10 (50)	8/13 (62)	ND
Blood test abnormality			
Coagulation defects	2/11 (18)	1/4 (25)	ND

NS, Noonan syndrome; LS, LEOPARD syndrome; ND, not described; TR, tricuspid regurgitation; PH, pulmonary hypertension; AS, aortic stenosis; PFO, patent foramen ovale; TOF, tetralogy of Fallot.
[a]Includes affected family members. Clinical manifestations in 3, 21, and 11 NS patients with *RAF1* mutations were summarized from three reports [Ko et al., 2008; Pandit et al., 2007; Razzaque et al., 2007], respectively.

rather broad. However, Western blotting using antineomycin phosphoacetyltransferase antibody that recognizes the amount of plasmids introduced in cells showed that the transfection efficiency in cells expressing p.S427G was similar to that in cells expressing other mutants (Fig. 2A). These findings were consistently observed in three independent experiments. Recent studies have shown that autophosphorylation of S621 is required to prevent proteasome-mediated degradation [Noble et al., 2008]. To explore the possibility that p.S427G mutant is resistant to proteasome-mediated degradation, we examined the amount of WT RAF1 and p.S427G at 24, 48, and 72 hr after transfection in serum-starved or complete medium (Fig. 2C). The results showed that the expression of Myc-tagged RAF1 in cells expressing p.S427G was similar to that in WT RAF1, although multiple bands were observed, suggesting the hyperphosphorylation of the p.S427G mutant.

ELK Transactivation in Mutant RAF1 Proteins

To examine the effect on the downstream pathway of mutant RAF1, we introduced five RAF1 mutants into NIH3T3 cells and examined ELK transactivation (Fig. 2D). ELK is a transcription factor, which is phosphorylated by activated ERK and then binds the serum response element in the promoter of the immediate-early genes, including *C-FOS*. ELK transactivation was enhanced in cells expressing p.S257L, p.N262K, and p.S427G without any stimulation, suggesting that these mutants were gain-of-function

Figure 1. Facial appearance of patients with *RAF1* mutations. **a–f:** patients with p.S257L mutations. **a:** NS135; **b:** NS146; **c:** NS215; **d:** NS256; **e:** NS258 at 6 months; **f:** 2 years and 4 months; **g:** NS222 with p.S427G. [Color figure can be viewed in the online issue, which is available at www.interscience.wiley.com.]

mutations. ELK transactivation in cells expressing p.H103G and p.R191I was not enhanced.

Phosphorylation State, ERK Activation, and Binding to the Scaffolding Protein 14-3-3 in Mutations in the CR2 Domain

Previous studies as well as the present study showed that mutations in NS-associated *RAF1* mutations were clustered in the CR2 domain. We hypothesized that amino acid changes in the CR2 domain impaired phosphorylation of serine at 259. We additionally generated expression construct harboring p.S259F and p.P261A substitutions, and their phosphorylation status was examined using anti-pRAF1 (S259) antibody together with RAF1 WT, p.S257L, p.N262K, and p.S427G (Fig. 3A). The results showed that phosphorylated proteins were scarcely observed in p.S257L, p.S259F, p.P261A, and p.N262K. Phosphorylation of ERK p44/42 was determined using anti-p-ERK (p44/42) antibody. All mutations activated the downstream ERK without any stimulation. The level of ERK phosphorylation in cells expressing mutants was lower than that in those treated with epidermal growth factor (EGF), suggesting that the expression of p.S257L, p.S259F, p.P261A, and p.N262K resulted in a partial activation of ERK.

Anti-pRAF1 (S259) antibody was produced by immunizing rabbits with a synthetic phospho-peptide corresponding to residues surrounding Ser259 of human RAF1. To examine if this antibody was able to recognize phosphorylation at S259 when mutations such as S257L and N262K were introduced, we performed a solid-phase immunoassay using biotinylated peptides as per the manufacturer's recommendation (Mimotopes, Victoria, Australia; Supp. Methods). The result showed that at least in peptides, this antibody could recognize serine phosphorylation in amino acid 259 when mutations S257L and N262K were introduced (Fig. 3B). These results support the data in Figure 3A, suggesting that S259 was not phosphorylated in mutants in the CR2 domain.

To examine if the RAF1 mutants without S259 phosphorylation were able to bind to 14-3-3, we cotransfected three double mutants (WT/S621A, S257L/S621A, and N262K/S621A) with FLAG-tagged 14-3-3, and coimmunoprecipitation was performed using anti-Myc antibody (Fig. 3C). The result showed that the WT/S621A mutant bound 14-3-3. In contrast, p.S257L/S621A and

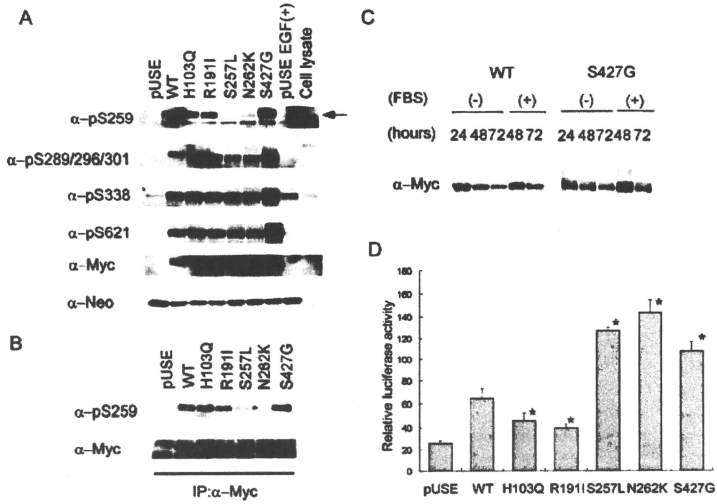

Figure 2. Analysis of phosphorylation status, degradation, and effect on downstream signaling in RAF1 mutants identified in this study. **A:** Phosphorylation status of wild-type (WT) RAF1 and mutants. Expression levels of RAF1 proteins and their phosphorylation levels were detected with different antibodies indicated in the figure. Transfection efficiency was measured using antineomycin phosphotransferase II (α-Neo) antibody. The arrow indicates the serine-phosphorylated expressed RAF1. **B:** Phosphorylation of S259 was confirmed by immunoprecipitation. Myc-tagged RAF1 was immunoprecipitated using anti-Myc antibody and the phosphorylation of S259 was determined. **C:** Time course experiments of WT RAF1 and p.S427G. The RAF1 protein was detected using anti-Myc antibody (clone 4A6; Millipore). FBS, fetal bovine serum. **D:** ELK transactivation in WT and mutants. Results are expressed as the means and standard deviations of mean values from triplicate samples. A significant increase in relative luciferase activity (RLA) was observed in cells transfected with p.S257L, p. N262K, and p.S427G, but not in cells transfected with p.H103Q or p.R191I. WT, wild-type; $^{*}P < 0.01$ by Student's *t*-test.

p.N262K/S621A mutants did not bind 14-3-3, suggesting that the decreased phosphorylation of S259 prevented 14-3-3 binding. A similar result was obtained in the coimmunoprecipitation study using anti-FLAG antibody (Fig. 3D). These results showed that mutants in the CR2 domain impaired phosphorylation of S259, abrogated the binding to 14-3-3 and resulted in a partial activation of ERK.

Discussion

In this study, we identified eight different *RAF1* mutations in 18 patients: p.S257L in 11 patients and p.R191I, p.S259F, p.P261A, p.P261L, p.N262K, p.S427G, and p.L613V in one patient each. Sixteen patients were diagnosed as having NS, although we were not able to reevaluate 2 patients with Costello syndrome. Examination of detailed clinical manifestations in the present study and past studies showed that patients with *RAF1* mutations were associated with hypertrophic cardiomyopathy, arrhythmia, and mental retardation. Results from previous studies and the present study showed 41/52 (79%) mutations to be located in the CR2 domain (Fig. 3E). We first demonstrated that mutations in the CR2 domain had impaired phosphorylation of S259. This caused the impaired binding of RAF1 to 14-3-3, resulting in a partial activation of downstream ERK. These results suggest that dephosphorylation of S259 is the primary mechanism of activation of mutant RAF1 located in the CR2 domain.

Phosphorylation of S259 and subsequent binding to 14-3-3 have been shown to be important for suppression of RAF1 activity [Dhillon et al., 2007]. Light et al. [2002] examined the phosphorylation status at S259 in the p.S257L mutant. Their experiment showed that phosphorylation of S259 still existed in the p.S257L mutant. The mutant was not able to bind 14-3-3 [Light et al., 2002]. In contrast, our functional studies demonstrated that all four mutants located in the CR2 domain (p.S257L, p.S259F, p.P261A, and p.N262K) impaired phosphorylation of S259 and that two of them impaired binding of 14-3-3. Impaired binding to 14-3-3 was also shown in p.P261S mutant [Pandit et al., 2007]. The reason for the difference on S259 phosphorylation between the result by Light et al. [2002] and ours is unclear. Enhanced kinase activities of mutants, including p.S257L, p.P261S, p.P261A, and p.V263A, were demonstrated in a previous study [Razzaque et al., 2007]. Phosphorylation levels at S338 in p.S257L and p.N262K were not enhanced compared to that in WT RAF1 (Fig. 2A), suggesting that the activation mechanism in these mutants is different from that of the normal state upon RAS-GTP binding. Indeed, ERK activation was partial compared with that in cells after EGF treatment (Fig. 3A). These results suggest that the conformational change around S259 due to amino acid changes results in the decreased phosphorylation of S259 and that mutant

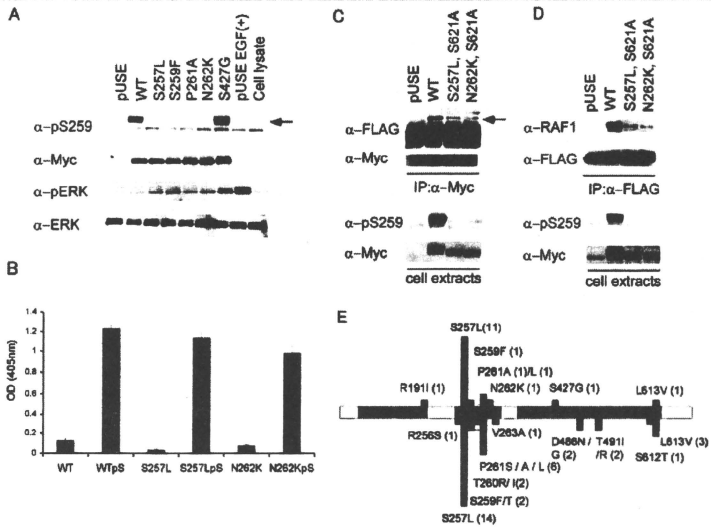

Figure 3. Phosphorylation of S259, binding to 14-3-3 and ERK activation of mutants located in the CR2 domain. **A:** Phosphorylation status of WT and mutants located in the CR2 domain. Phosphorylation of S259 was not observed in cells expressing p.S257L, p.S259F, p.P261A, and p.N262K. In order to examine the level of full activation of ERK, mock-transfected cells were treated with 10 ng/ml EGF. ERK activation was observed in cells expressing p.S257L, p.S259F, p.P261A, and p.N262K, but was weaker than those in cells expressing p.S427G and EGF-treated cells. The arrow indicates the serine-phosphorylated expressed RAF1. **B:** Epitope mapping of the anti-pRAF1 (S259) antibody using a solid-phase immunoassay. The antibody was able to recognize peptides with S257L or N262K mutations when S259 was phosphorylated, but was not able to recognize peptides without Ser259 phosphorylation. Results are expressed as the means and standard deviations of mean values from triplicate samples. **C:** Binding of RAF-1 to 14-3-3ζ. HEK293 cells were transfected with constructs harboring FLAG-tagged 14-3-3 and one construct of pUSE WT, p.S257L/p.S621A, or p.N262K/ p.S621A. Immunoprecipitation was performed using anti-Myc antibody, and 14-3-3 binding was determined by anti-FLAG antibody (upper panel). Phosphorylation of S259 and RAF1 expression were determined in cell lysates used for the immunoprecipitation (lower panel). The arrow indicates the band for 14-3-3. **D:** Binding of 14-3-3ζ to RAF-1. Immunoprecipitation was performed using anti-FLAG antibody and RAF1 binding was examined using anti-RAF1 antibody (upper panel). The binding of 14-3-3 to endogenous RAF1 was scarcely observed (lane 1, pUSE). Phosphorylation of S259 and RAF1 expression were determined using cell lysates used for the immunoprecipitation (lower panel). **E:** Domain organization and the distribution of mutations in RAF1 protein. The three regions conserved in all RAF proteins (conserved region [CR] 1, CR2, and CR3) are shown in pink. Mutations identified in this study are shown above the bar and those reported before [Ko et al. 2008; Pandit et al. 2007; Razzaque et al. 2007] are shown below the bar. Green squares indicate families with NS. Orange squares indicate patients with LEOPARD syndrome and the yellow square indicates a patient with hypertrophic cardiomyopathy.

RAF-1 then dissociates from 14-3-3; the substrate would thus be targeted to the catalytic domain in the CR3 domain (Fig. 4).

To highlight the clinical pictures of patients with *RAF1* mutations, clinical manifestations in 52 patients with *RAF1* mutations [Ko et al., 2008; Pandit et al., 2007; Razzaque et al., 2007], 172 patients with *PTPN11* mutations [Jongmans et al., 2005; Musante et al., 2003; Tartaglia et al., 2002; Zenker et al., 2004], 73 patients with *SOS1* mutations [Ferrero et al., 2008; Narumi et al., 2008; Roberts et al., 2007; Tartaglia et al., 2007; Zenker et al., 2007a] and 18 patients with *KRAS* mutations [Carta et al., 2006; Ko et al., 2008; Lo et al., 2008; Schubbert et al., 2006; Zenker et al., 2007b] are summarized in Table 3. The frequency of perinatal abnormalities was similar between patients with *RAF1* and *SOS1*. In contrast, the description of perinatal abnormalities was rare in patients with *PTPN11* and *KRAS* mutations. Growth failure and mental retardation were observed in 100 and 94% of NS with *KRAS* mutations, respectively. Growth failure and mental retardation were observed in 87 and 56% of patients with *RAF1* mutations, respectively. In contrast, those manifestations were less frequent (63 and 43%) in patients with *PTPN11* mutations. The frequency of mental retardation was lowest in patients with *SOS1* mutations (18%). We were unable to compare gene-specific features in craniofacial characteristics because such details were not described in the previous reports. As for skeletal characteristics, short stature was frequently manifested in patients with *RAF1* mutations (82%) followed by *KRAS* mutation-positive patients (71%). The association of short stature was lower in *PTPN11* mutation-positive and *SOS1* mutation-positive patients (56 and 38%, respectively). It is noteworthy that the association of hypertrophic cardiomyopathy was specifically high (73%) in *RAF1* mutation-positive patients. In contrast, hypertrophic cardiomyopathy was observed in 20% of clinically diagnosed Noonan

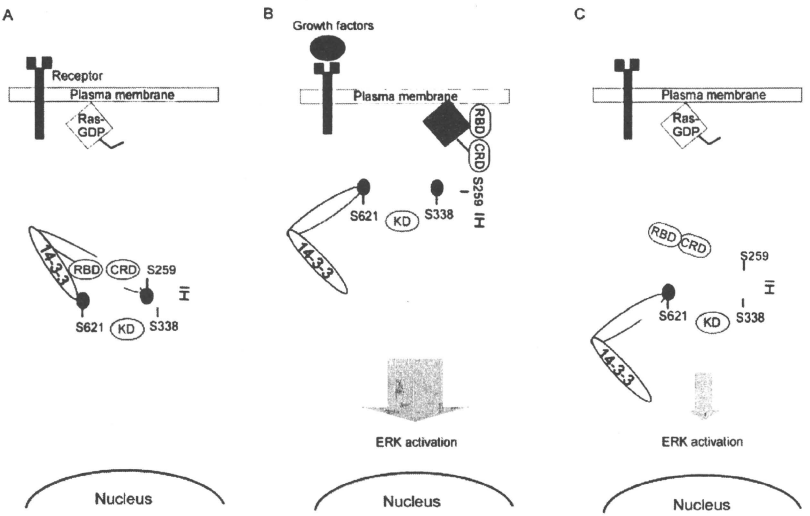

Figure 4. Schematic model of WT and mutant activation. **A:** In an inactive state, RAF1 is phosphorylated on S259 and S621 and is bound to 14-3-3. **B:** In growth-factor stimulation, the GTP-bound RAS binds to the CR1 domain of RAF1, which displaces 14-3-3. S259 is dephosphorylated by protein phosphatase 1 (PP1) and/or protein phosphatase 2A (PP2A). After RAF1 is recruited to the plasma membrane, phosphorylation of S338, Y341, T491, and S494 occurs. The phosphorylation of these residues is thought to be important for the full activation of RAF1. **C:** Mutants whose amino acid changes are located in the CR2 domain. It has been reported that S259 was phosphorylated by Akt and dephosphorylated by PP1 and/or PP2A. Amino acid changes in the CR2 domain would cause structural changes in the CR2 domain, leading to the access of PP2A to S259. Alternatively, Akt kinase would not be able to phosphorylate S259. S259 is dephosphorylated without stimulation and substrate(s) would be able to enter the kinase domain, leading to a partial activation. RBD, RAS-binding domain; CRD, cysteine-rich domain; KD, kinase domain; IH, isoform-specific hinge segment region. [Color figure can be viewed in the online issue, which is available at www.interscience.wiley.com.]

patients [van der Burgt 2007] and in 7, 10, and 17% of patients with *PTPN11*, *SOS1*, and *KRAS* mutations, respectively. These results strongly suggest that patients with *RAF1* mutations have a significantly higher risk of hypertrophic cardiomyopathy. Mitral valve abnormality and arrhythmia were also frequently observed in patients with *RAF1* mutations (27 and 56%, respectively). In summary, these results highlight specific manifestations of patients with *RAF1* mutations: high frequency of hypertrophic cardiomyopathy, septal defects of the heart, short stature, and less frequent PS (Supp. Fig. S1). The high frequency of heart defects would be associated with a high risk of sudden death in *RAF1* mutation-positive patients.

The present study is the first to identify p.S427G in a patient with NS. The same mutation has been reported in a patient with therapy-related acute myeloid leukemia [Zebisch et al., 2006]. The patient reported by Zebisch et al. [2006] first developed immature teratoma, yolk sack tumor, and embryonal testicular carcinoma. Thirty-five months after tumor resection and chemotherapy, the patient developed acute myeloid leukemia. Molecular analysis of *RAF1* revealed the de novo p.S427G mutation in leukemia cells and DNA from buccal epithelial cells [Zebisch et al., 2006]. Whether or not the patient had an NS phenotype was not mentioned. *RAF1* mutations have been rarely reported in malignant tumors. As far as we could determine, only six mutations, including p.P207S, p.V226I, p.Q335H, p.S427G, p.I448V, and p.E478K, have been identified in tumors and therapy-related leukemias [Pandit et al., 2007; Razzaque et al., 2007]. A previous study as well as our results showed that p.S427G mutant has transformation capacity [Zebisch et al., 2009], is resistant to apoptosis when introduced into NIH3T3 cells [Zebisch et al., 2009] and activates ERK and ELK transcription, suggesting that p.S427G is a gain-of-function mutation. We identified p.S427G in a familial case of NS. The mother and boy have not yet developed malignant tumors. Although no NS patients with *RAF1* mutations have developed malignant tumors, careful observation might be prudent in *RAF1* mutation-positive children.

We identified two novel mutations, p.R191I and p.N262K. p.R191I is located in the CR1, and arginine at amino acid position 191 is evolutionally conserved [Mercer and Pritchard, 2003]. Activation of ERK was not observed in cells expressing p.R191I. ELK transactivation was rather decreased; parental samples were not available. There is a possibility that this change is a polymorphism.

In conclusion, we identified *RAF1* mutations in 18 patients and detailed clinical manifestations in mutation-positive patients were examined. Our analysis of patients with mutations in *RAF1*, *PTPN11*, *SOS1*, and *KRAS* showed hypertrophic cardiomyopathy and short stature to be frequently observed in patients with *RAF1* mutations. Functional analysis revealed that dephosphorylation of S259 would be the essential mechanism for ERK activation in RAF1 mutations. Despite recent progress in molecular characterization of NS and related disorders, genetic causes in

Table 3. Clinical Manifestations in NS Patients with *RAF1, PTPN11, SOS1,* and *KRAS* Mutations

	RAF1[a] (%)	PTPN11[b] (%)	SOS1[c] (%)	KRAS[d] (%)
Total patients	52	172	73	18
Perinatal abnormality				
Polyhydramnios	12/34 (35)	ND	9/16 (56)	2
Fetal macrosomia	11/31 (35)	ND	9/15 (60)	ND
Growth and development				
Failure to thrive in infancy	13/15 (87)	35/56 (63)	ND	3/3 (100)
Mental retardation	25/45 (56)	71/164 (43)	12/67 (18)[e]	16/17 (94)[f]
Outcome				
Died	6/28 (21)	ND	ND	ND
Craniofacial characteristics				
Relative macrocephaly	32/38 (84)	ND	9/21 (43)[e]	9/11 (82)
Hypertelorism	34/36 (94)	15/28 (54)[e]	5/6 (83)	12/12 (100)
Downslanting palpebral fissures	29/37 (78)	19/28 (68)	20/22 (91)	9/12 (75)
Ptosis	28/37 (76)	18/29 (62)	19/24 (79)	10/15 (67)
Epicanthal folds	24/35 (69)	15/28 (54)	ND	2/9 (22)[e]
Low set ears	32/36 (89)	56/64 (88)	20/22 (91)	7/10 (70)
Skeletal characteristics				
Short stature	41/50 (82)	97/172 (56)[e]	22/58 (38)[e]	12/17 (71)
Short neck	35/46 (76)	15/29 (52)[e]	17/22 (77)	9/10 (90)
Webbing of neck	38/46 (83)	36/122 (30)[e]	3/6 (50)	7/14 (50)[e]
Cardiac defects				
Hypertrophic cardiomyopathy	37/51 (73)	10/135 (7)[e]	7/73 (10)[e]	3/18 (17)[e]
Septal defect	22/52 (42)	41/170 (24)[e]	17/73 (23)[e]	5/18 (28)
Atrial septal defect	16/51 (31)			4/18 (22)
Ventricular septal defect	6/52 (12)			1/18 (6)
Pulmonic stenosis	11/50 (22)	125/171 (73)[f]	53/73 (73)[f]	7/18 (39)
Patent ductus arteriosus	2/20 (10)	ND	ND	1/18 (6)
Mitral valve anomaly	13/49 (27)	ND	ND	3/18 (17)
Arrhythmia	14/25 (56)	ND	ND	ND
Skeletal/extremity deformity				
Cubitus valgus	9/31(29)	14/61 (23)	1/6 (17)	2/2 (100)
Pectus deformity	25/44 (57)	108/171 (63)	38/56 (68)	13/16 (81)
Skin/hair anomaly				
Curly hair	14/41 (34)	ND	15/22 (68)[f]	1/12 (8)
Hyperelastic skin	12/33 (36)	ND	1/6 (17)	3/12 (25)
Cafe au lait spots	3/34 (9)	ND	1/6 (17)	1/9 (11)
Lentigines	3/35 (9)	ND	ND	ND
Naevus	12/37 (32)	ND	ND	ND
Genitalia				
Cryptorchidism	13/23 (57)	75/138 (54)	22/39 (56)	4/11 (36)
Blood test abnormality				
Coagulation defects	3/15 (20)	46/90 (51)	14/66 (21)	2/9 (22)

ND, not described.
[a][Ko et al., 2008; Pandit et al., 2007; Razzaque et al., 2007]; and this study.
[b][Jongmans et al., 2005; Musante et al., 2003; Tartaglia et al., 2002; Zenker et al., 2004].
[c][Ferrero et al., 2008; Ko et al., 2008; Narumi et al., 2008; Roberts et al., 2007; Tartaglia et al., 2007; Zenker et al., 2007a].
[d][Carta et al., 2006; Ko et al., 2008; Lo et al., 2008; Schubbert et al., 2006; Zenker et al., 2007b].
[e]The frequency of the manifestation in patients with the gene was significantly lower compared with that observed in *RAF1*-positive patients ($P < 0.05$ by Fisher's exact test).
[f]The frequency of the manifestation in patients with the gene was significantly higher compared with that observed in *RAF1*-positive patients ($P < 0.05$ by Fisher's exact test).

approximately 30% of NS and related disorders remain unknown. Presently unknown genetic causes for mutation-negative NS and related disorders remain to be identified in molecules in future studies.

Acknowledgments

The authors wish to thank the patients and their families who participated in this study. We are grateful to physicians who referred the patients and to Kumi Kato and Miyuki Tsuda for technical assistance. This work was supported by Grants-in-Aids from the Ministry of Education, Culture, Sports, Science and Technology of Japan, Japan Society for the Promotion of Science, and The Ministry of Health Labour and Welfare to Y.M. and Y.A. and by an outstanding Senior Graduate Student award from Tohoku University Graduate School of Medicine to T.K.

References

Allanson JE, Hall JG, Hughes HE, Preus M, Witt RD. 1985. Noonan syndrome: the changing phenotype. Am J Med Genet 21:507–514.

Aoki Y, Niihori T, Kawame H, Kurosawa K, Ohashi H, Tanaka Y, Filocamo M, Kato K, Suzuki Y, Kure S, Matsubara Y. 2005. Germline mutations in HRAS proto-oncogene cause Costello syndrome. Nat Genet 37:1038–1040.

Aoki Y, Niihori T, Narumi Y, Kure S, Matsubara Y. 2008. The RAS/MAPK syndromes: novel roles of the RAS pathway in human genetic disorders. Hum Mutat 29:992–1006.

Bentires-Alj M, Kontaridis MI, Neel BG. 2006. Stops along the RAS pathway in human genetic disease. Nat Med 12:283–285.

Brems H, Chmara M, Sahbatou M, Denayer E, Taniguchi K, Kato R, Somers R, Messiaen L, De Schepper S, Fryns JP, Cools J, Marynen P, Thomas G, Yoshimura A, Legius E. 2007. Germline loss-of-function mutations in SPRED1 cause a neurofibromatosis 1-like phenotype. Nat Genet 39:1120–1126.

Carta C, Pantaleoni F, Bocchinfuso G, Stella L, Vasta I, Sarkozy A, Digilio C, Palleschi A, Pizzuti A, Grammatico P, Zampino G, Dallapiccola B, Gelb BD, Tartaglia M. 2006. Germline missense mutations affecting KRAS isoform B are associated with a severe Noonan syndrome phenotype. Am J Hum Genet 79:129–135.

Dhillon AS, von Kriegsheim A, Grindlay J, Kolch W. 2007. Phosphatase and feedback regulation of Raf-1 signaling. Cell Cycle 6:3–7.

Digilio MC, Conti E, Sarkozy A, Mingarelli R, Dottorini T, Marino B, Pizzuti A, Dallapiccola B. 2002. Grouping of multiple-lentigines/LEOPARD and Noonan syndromes on the PTPN11 gene. Am J Hum Genet 71:389–394.

Ferrero GB, Baldassarre G, Delmonaco AG, Biamino E, Banaudi E, Carta C, Rossi C, Silengo MC. 2008. Clinical and molecular characterization of 40 patients with Noonan syndrome. Eur J Med Genet 51:566–572.

Hennekam RC. 2003. Costello syndrome: an overview. Am J Med Genet C Semin Med Genet 117:42–48.

Jongmans M, Sistermans EA, Rikken A, Nillesen WM, Tamminga R, Patton M, Maier EM, Tartaglia M, Noordam K, van der Burgt I. 2005. Genotypic and phenotypic characterization of Noonan syndrome: new data and review of the literature. Am J Med Genet A 134A:165–170.

Ko JM, Kim JM, Kim GH, Yoo HW. 2008. PTPN11, SOS1, KRAS, and RAF1 gene analysis, and genotype–phenotype correlation in Korean patients with Noonan syndrome. J Hum Genet 53:999–1006.

Light Y, Paterson H, Marais R. 2002. 14-3-3 antagonizes Ras-mediated Raf-1 recruitment to the plasma membrane to maintain signaling fidelity. Mol Cell Biol 22:4984–4996.

Lo FS, Lin JL, Kuo MT, Chiu PC, Shu SG, Chao MC, Lee YJ, Lin SP. 2008. Noonan syndrome caused by germline KRAS mutation in Taiwan: report of two patients and a review of the literature. Eur J Pediatr 168:919–923.

Mendez HM, Opitz JM. 1985. Noonan syndrome: a review. Am J Med Genet 21:493–506.

Mercer KE, Pritchard CA. 2003. Raf proteins and cancer: B-Raf is identified as a mutational target. Biochim Biophys Acta 1653:25–40.

Musante L, Kehl HG, Majewski F, Meinecke P, Schweiger S, Gillessen-Kaesbach G, Wieczorek D, Hinkel GK, Tinschert S, Hoeltzenbein M, Ropers HH, Kalscheuer VM. 2003. Spectrum of mutations in PTPN11 and genotype–phenotype correlation in 96 patients with Noonan syndrome and five patients with cardio-facio-cutaneous syndrome. Eur J Hum Genet 11:201–206.

Narumi Y, Aoki Y, Niihori T, Sakurai M, Cave H, Verloes A, Nishio K, Ohashi H, Kurosawa K, Okamoto N, Kawame H, Mizuno S, Kondoh T, Addor MC, Coeslier-Dieux A, Vincent-Delorme C, Tabayashi K, Aoki M, Kobayashi T, Guliyeva A, Kure S, Matsubara Y. 2008. Clinical manifestations in patients with SOS1 mutations range from Noonan syndrome to CFC syndrome. J Hum Genet 53:834–841.

Niihori T, Aoki Y, Narumi Y, Neri G, Cave H, Verloes A, Okamoto N, Hennekam RC, Gillessen-Kaesbach G, Wieczorek D, Kavamura MI, Kurosawa K, Ohashi H, Wilson L, Heron D, Bonneau D, Corona G, Kaname T, Naritomi K, Baumann C, Matsumoto N, Kato K, Kure S, Matsubara Y. 2006. Germline KRAS and BRAF mutations in cardio-facio-cutaneous syndrome. Nat Genet 38:294–296.

Noble C, Mercer K, Hussain J, Carragher L, Giblett S, Hayward R, Patterson C, Marais R, Pritchard CA. 2008. CRAF autophosphorylation of serine 621 is required to prevent its proteasome-mediated degradation. Mol Cell 31:862–872.

Pandit B, Sarkozy A, Pennacchio LA, Carta C, Oishi K, Martinelli S, Pogna EA, et al. 2007. Gain-of-function RAF1 mutations cause Noonan and LEOPARD syndromes with hypertrophic cardiomyopathy. Nat Genet 39:1007–1012.

Razzaque MA, Nishizawa T, Komoike Y, Yagi H, Furutani M, Amo R, Kamisago M, Momma K, Katayama H, Nakagawa M, Fujiwara Y, Matsushima M, Mizuno K, Tokuyama M, Hirota H, Muneuchi J, Higashinakagawa T, Matsuoka R. 2007. Germline gain-of-function mutations in RAF1 cause Noonan syndrome. Nat Genet 39:1013–1017.

Reynolds JF, Neri G, Herrmann JP, Blumberg B, Coldwell JG, Miles PV, Opitz JM. 1986. New multiple congenital anomalies/mental retardation syndrome with cardio-facio-cutaneous involvement—the CFC syndrome. Am J Med Genet 25:413–427.

Roberts AE, Araki T, Swanson KD, Montgomery KT, Schiripo TA, Joshi VA, Li L, Yassin Y, Tamburino AM, Neel BG, Kucherlapati RS. 2007. Germline gain-of-function mutations in SOS1 cause Noonan syndrome. Nat Genet 39: 70–74.

Rodriguez-Viciana P, Tetsu O, Tidyman WE, Estep AL, Conger BA, Cruz MS, McCormick F, Rauen KA. 2006. Germline mutations in genes within the MAPK pathway cause cardio-facio-cutaneous syndrome. Science 311:1287–1290.

Schubbert S, Zenker M, Rowe SL, Boll S, Klein C, Bollag G, van der Burgt I, Musante L, Kalscheuer V, Wehner LE, Nguyen H, West B, Zhang KY, Sistermans E, Rauch A, Niemeyer CM, Shannon K, Kratz CP. 2006. Germline KRAS mutations cause Noonan syndrome. Nat Genet 38:331–336.

Tartaglia M, Kalidas K, Shaw A, Song X, Musat DL, van der Burgt I, Brunner HG, Bertola DR, Crosby A, Ion A, Kucherlapati RS, Jeffery S, Patton MA, Gelb BD. 2002. PTPN11 mutations in Noonan syndrome: molecular spectrum, genotype-phenotype correlation, and phenotypic heterogeneity. Am J Hum Genet 70: 1555–1563.

Tartaglia M, Mehler EL, Goldberg R, Zampino G, Brunner HG, Kremer H, van der Burgt I, Crosby AH, Ion A, Jeffery S, Kalidas K, Patton MA, Kucherlapati RS, Gelb BD. 2001. Mutations in PTPN11, encoding the protein tyrosine phosphatase SHP-2, cause Noonan syndrome. Nat Genet 29:465–468.

Tartaglia M, Pennacchio LA, Zhao C, Yadav KK, Fodale V, Sarkozy A, Pandit B, Oishi K, Martinelli S, Schackwitz W, Ustaszewska A, Martin J, Bristow J, Carta C, Lepri F, Neri C, Vasta I, Gibson K, Curry CJ, Siguero JP, Digilio MC, Zampino G, Dallapiccola B, Bar-Sagi D, Gelb BD. 2007. Gain-of-function SOS1 mutations cause a distinctive form of Noonan syndrome. Nat Genet 39:75–79.

van der Burgt I. 2007. Noonan syndrome. Orphanet J Rare Dis 2:4.

Zebisch A, Haller M, Hiden K, Goebel T, Hoefler G, Troppmair J, Sill H. 2009. Loss of RAF kinase inhibitor protein is a somatic event in the pathogenesis of therapy-related acute myeloid leukemias with C-RAF germline mutations. Leukemia 23:1049–1053.

Zebisch A, Staber PB, Delavar A, Bodner C, Hiden K, Fischereder K, Janakiraman M, Linkesch W, Auner HW, Emberger W, Windpassinger C, Schimek MG, Hoefler G, Troppmair J, Sill H. 2006. Two transforming C-RAF germ-line mutations identified in patients with therapy-related acute myeloid leukemia. Cancer Res 66:3401–3408.

Zenker M, Buheitel G, Rauch R, Koenig R, Bosse K, Kress W, Tietze HU, Doerr HG, Hofbeck M, Singer H, Reis A, Rauch A. 2004. Genotype–phenotype correlations in Noonan syndrome. J Pediatr 144:368–374.

Zenker M, Horn D, Wieczorek D, Allanson J, Pauli S, van der Burgt I, Doerr HG, Gaspar H, Hofbeck M, Gillessen-Kaesbach G, Koch A, Meinecke P, Mundlos S, Nowka A, Rauch A, Reif S, von Schnakenburg C, Seidel H, Wehner LE, Zweier C, Bauhuber S, Matejas V, Kratz CP, Thomas C, Kutsche K. 2007a. SOS1 is the second most common Noonan gene but plays no major role in cardio-facio-cutaneous syndrome. J Med Genet 44:651–656.

Zenker M, Lehmann K, Schulz AL, Barth H, Hansmann D, Koenig R, Korinthenberg R, Kreiss-Nachtsheim M, Meinecke P, Morlot S, Mundlos S, Quante AS, Raskin S, Schnabel D, Wehner LE, Kratz CP, Horn D, Kutsche K. 2007b. Expansion of the genotypic and phenotypic spectrum in patients with KRAS germline mutations. J Med Genet 44:131–135.

Non-Hodgkin Lymphoma in a Patient With Cardiofaciocutaneous Syndrome

Akira Ohtake, MD, PhD, Yoko Aoki, MD, PhD,† Yuka Saito, MD,† Tetsuya Niihori, MD, PhD,† Atsushi Shibuya, MD, PhD,* Shigeo Kure, MD, PhD,† and Yoichi Matsubara, MD†*

Summary: Cardiofaciocutaneous (CFC) syndrome is a multiple congenital anomaly/mental retardation syndrome characterized by a distinctive facial appearance, ectodermal abnormalities, and heart defects. Clinically, it overlaps with both Noonan syndrome and Costello syndrome. Mutations in KRAS, BRAF, and MAP2K1/2 (MEK1/2) have been identified in patients with CFC syndrome. BRAF mutations are involved in more than 80% of CFC syndrome patients, and we have reported earlier that 2 CFC patients with BRAF mutations developed acute lymphoblastic leukemia. Here we report a boy with CFC syndrome who developed non-Hodgkin lymphoma. At 2 months of age, he developed pneumonia with pleurisy and was diagnosed as having non-Hodgkin lymphoma (precursor T-cell lymphoblastic lymphoma) by cytopathologic examination of the pleural fluid. He was suspected of having Noonan syndrome because of his facial appearance, webbed neck, and cubitus valgus. Precursor T-cell lymphoblastic lymphoma was treated by the TCCSG NHL 94-04 protocol. At 9 years of age, he was clinically reevaluated and diagnosed as having CFC syndrome because of his distinctive facial appearance, multiple nevi, and moderate mental retardation. Sequencing analysis showed a germline p.A246P (c.736G > C) mutation in BRAF reported earlier in CFC syndrome. Molecular diagnosis and careful observation should be considered in children with CFC syndrome.

Key Words: RAF, RAS-MAPK, non-Hodgkin lymphoma, cardiofaciocutaneous syndrome, Noonan syndrome, KRAS, BRAF, leukemia

(*J Pediatr Hematol Oncol* 2010;00:000–000)

Cardiofaciocutaneous (CFC) syndrome is a multiple congenital anomaly/mental retardation syndrome characterized by heart defects, facial dysmorphism, ectodermal abnormalities, and mental retardation.[1,2] Typical facial characteristics include a high forehead with bitemporal constriction, hypoplastic supraorbital ridges, downslanting palpebral fissures, a depressed nasal bridge, and posteriorly angulated ears with prominent helices. Affected individuals present with heart defects, including pulmonic stenosis, atrial septal defects, and hypertrophic cardiomyopathy. Ectodermal abnormalities including sparse, friable hair, multiple nevi, and hyperkeratotic skin lesions are noted. CFC syndrome has many clinical features in common with those of Noonan syndrome and Costello syndrome. Of these 3 syndromes, Noonan syndrome is most frequent, its incidence is estimated to be 1 in 1000 to 1 in 2500 live births. Compared with the other 2 syndromes, Noonan syndrome has lower frequencies of mental retardation (24% to 35%), heart defects (50% to 67%), and skin abnormalities (2% to 27%),[3] whereas CFC patients show a high frequency of growth failure (78.9%), mental retardation (100%), heart defects (84.2%), and skin abnormalities (68.4%).[2] Costello syndrome is characterized by mental retardation, high birth weight, neonatal feeding problems, curly hair, redundant skin, nasal papillomata, and tumor predisposition. Wrinkled palms and soles, hyperpigmentation, and joint hyperextension, which have been commonly reported in Costello syndrome but not in CFC syndrome, have been observed in 30% to 40% of the mutation-positive CFC patients.[4] Thus, differential diagnosis of these syndromes is difficult because of their overlapping clinical manifestations.

Mutations in molecules in the RAS/mitogen-activated protein kinase (MAPK) pathway have been identified in these disorders: HRAS in Costello syndrome[5]; *PTPN11*, *KRAS*, *SOS1*, *RAF1*, and *NRAS* in Noonan syndrome[6–12]; and *KRAS*, *BRAF*, and *MAP2K1/2* in individuals with CFC syndrome.[2,13] Therefore, these syndromes are termed NCFC syndrome or RAS/MAPK syndromes.[14,15] Approximately 10% of patients with Costello syndrome have been shown to have malignant tumors, including neuroblastoma, rhabdomyosarcoma, and bladder carcinoma. For Costello syndrome, tumor-screening protocols have been proposed.[16] In contrast, little attention has been paid to the development of tumors in patients with CFC syndrome.

Herein we report a Japanese patient with CFC syndrome who developed non-Hodgkin lymphoma (NHL) at 2 months of age. Although he had been suspected of having Noonan syndrome, reevaluation of the clinical manifestations and identification of a BRAF mutation led to a rediagnosis of CFC syndrome. Our observations, together with a literature review of earlier patients, suggest the importance of the careful observation for malignancy in CFC syndrome.

CASE REPORT

The propositus was a 12-year-old Japanese boy. He was the first son of unrelated healthy parents. At birth, his father was 27 years old, as was his mother. The baby was delivered at 40 weeks by obstetrical vacuum extraction and its birth weight was 3488 g (+0.8 SD), length was 49.6 cm (+0.1 SD), and occipitofrontal circumference was 35 cm (+1.0 SD). At 2 months of age, coughing, rhinorrhea, and feeding difficulty were observed. He was admitted

Received for publication October 29, 2009; accepted February 19, 2010.
From the *Department of Pediatrics, Saitama Medical University, Moroyama, Saitama; and †Department of Medical Genetics, Tohoku University School of Medicine, Sendai, Japan.
This work was supported by grants-in-aid from Japan Society for the Promotion of Science and from the Ministry of Health, Labor, and Welfare of Japan. The authors have no financial interest in the outcome of this study.
Reprints: Yoko Aoki, MD, PhD, Department of Medical Genetics, Tohoku University School of Medicine, 1-1 Seiryo-machi, Sendai 980-8574, Japan (e-mail: aokiy@mail.tains.tohoku.ac.jp).

to our hospital because his chest roentgenogram showed right lung pneumonia with pleurisy. Echocardiography was normal and a computed tomography scan showed right atelectasis and right pleural effusion. There were no mediastinal or axillary lymphadenopathies. Laboratory findings were as follows: hemoglobin 10.4 g/dL, white blood cells 9.1×10^9/L, and platelets 404×10^9/L. The levels of serum lactate dehydrogenase and C-reactive protein were normal. Pleural effusion aspirate had a milky-white appearance, a triglyceride content of 2529 mg/dL, and a lactate dehydrogenase level of 1656 IU/dL. Cytologic examination of the pleural fluid showed highly cellular specimens. The majority of these cells were lymphoblasts. These cells showed T-cell phenotype: positive for CD2, CD3, CD5, and CD7 by an immunophenotyping study using flow cytometry. No other infiltration was identified by computed tomography /magnetic resonance imaging, bone marrow aspiration, and Garium scintigram. He was then diagnosed as having T-cell lymphoblastic lymphoma by cytopathologic examination of the pleural fluid (stage III). At admission, the patient was diagnosed as having Noonan syndrome because of the following anomalies: hypertelorism, downslanting palpebral fissures, low nasal bridge, low set and posterior rotated ears, micrognathia, short and webbed neck, cubitus vulgus, funnel chest, and wide nipples. His chromosomal analyses of both peripheral lymphocytes and lymphoma cells showed a normal karyotype of 46, XY.

Induction therapy, which consisted of vincristine, predonisolone, tetrahydropyranyl adriamycin, cyclophosphamide, and *Escherichia coli* asparaginase, was performed for 3 months. The patient had a good clinical response to the chemotherapy, which was terminated before the entire protocol was finished. No relapse was observed afterwards.

At the age of 9 years, he had a distinctive facial appearance, including hypertelorism, underdeveloped supraorbital ridges, sparse and highly arched eyebrows, bilateral ptosis, depressed nasal bridge, concave nasal ridge, broad nasal base, anteverted nares, long philtrum, everted lower lip, and low set and posterior rotated ears (Fig. 1). Other features included a webbed/short neck, multiple nevi in his face, cubitus valgus, pectus excavatum, widely spaced nipples, and short stature of −3.1 SD. Results of growth hormone provocation tests with arginine and insulin were both normal. Echocardiography and ECG revealed no cardiac abnormalities. His intelligent quotient has not been accurately examined, but he attends a class for the handicapped. At 9 years of age, he was suspected of having CFC syndrome because of his facial appearance, mental retardation, and multiple nevi, although no heart defects were noted.

FIGURE 1. Facial appearance of the patient.

Mutation Analysis

Genomic DNA from blood leukocytes from the patient was isolated by a standard protocol. Fifteen exons with flanked introns in which the mutations have been identified in CFC patients and *HRAS* exon1, in which mutations are clustered in more than 90% of patients with Costello syndrome, were examined and amplified by polymerase chain reaction. These were exons 1, 2, and 5 in *KRAS*; exons 6 and 11 to 16 in *BRAF*; exons 2 and 3 in *MAP2K1*; and exons 2, 3, and 7 in *MAP2K2*.[2,4] The polymerase chain reaction products were gel purified and sequenced on an ABI PRISM 310 automated DNA sequencer (Applied Biosystems). This study was approved by the Ethics Committee of the Tohoku University School of Medicine. We obtained informed consent for the sample and specific consent for a photograph. Sequencing analysis showed a G-to-C change at nucleotide 736, resulting in an A246P mutation of BRAF in the heterozygous form.

DISCUSSION

The patient with CFC syndrome herein reported developed right lung pneumonia with pleurisy at 2 months of age. He was first diagnosed as having Noonan syndrome. The cytopathologic examination of lymphoblasts in the pleural fluid showed T-cell phenotype and the patient was diagnosed as having precursor T-cell lymphoblastic lymphoma. At 9 years of age, a *BRAF* A246P mutation was identified in the patient. We concluded that the patient had CFC syndrome because of his distinctive facial features, including underdeveloped supraorbital ridges, sparse and highly arched eyebrows, ptosis, growth failure, moderate mental retardation, and multiple nevi in skin, although no heart defects were observed.

Mutations in *BRAF* identified in CFC patients partially overlap those identified in cancers. V600E mutation, which is most frequently identified in cancers, has never been detected in CFC patients and activation of downstream extracellular signal-regulated kinase is weaker in germline mutations than in V600E.[15] The association with malignancy is rarer in CFC syndrome than in Costello syndrome with germline *HRAS* mutations, 10% of which develop malignant tumors including rhabdomyosarcoma, neuroblastoma, and bladder carcinoma. Four patients with CFC syndrome have been found to develop malignant tumors (Table 1). We have earlier reported 2 patients with *BRAF* mutations who developed acute lymphoblastic leukemia (ALL).[2,18] A CFC patient with a MEK1 mutation has been reported to have developed hepatoblastoma after cardiac transplantation.[19] To date, 104 CFC patients with *BRAF* mutations and 42 with CFC patients with MEK1/2 mutations have been reported.[15] The frequency of the association with malignant tumors cannot be neglected. Careful observation should be considered in children with CFC syndrome and related disorders.

Precursor T-cell lymphoblastic lymphoma accounts for approximately 33% of pediatric NHL and most commonly involves the mediastinum and lymph nodes.[20] The precise incidence of NHL in children is not known and the development of NHL in the early infantile period is rare.[21] It is possible that our patient developed NHL at 2 months of age owing to having the germline mutation in the proto-oncogene *BRAF*.

The contribution of somatic mutations in BRAF to hematologic malignancy has been controversial. Lee et al[22] identified BRAF mutations in 4 cases with diffuse large

TABLE 1. Summary of CFC Patients who Developed Malignant Tumors

	1[2,17]	2[18]	3 (Current Study)	4[19]
Gene	*BRAF*	*BRAF*	*BRAF*	MEK1
Amino acid change	G469E	E501G	A246P	Y130C
Clinical manifestations				
Clinical diagnosis	CFC	CFC	Noonan (2 months of age), CFC (9 y)	Costello (6 wk) CFC
Heart defects	Mild PS, ASD, and asymmetrical hypertrophy of the interventricular septum	Patent ductus arteriosus and asymmetrical hypertrophy of the interventricular septum	No	Heart transplantation owing to severe hypertrophic cardiomyopathy (8 mo of age), a small anterior muscular septal defect
Skin and hair	Keratosis pilaris (3 y) cafe au lait spots, sparse, friable hair	Generalized pigmentation and patchy hyperkeratosis, sparse curly hair	Multiple nevi (9 y)	Loose plantar and palmer skin with deep creases, sparse thin hair
Mental and growth development	Moderate mental retardation	Severe mental retardation	Moderate mental retardation, short stature (−3.1 SD)	Developmental delay
Other		Bilateral cryptorchidism		
Hematologic malignancy	ALL	ALL	Precursor T-lymphoblastic lymphoma	Hepatoblastoma
Age at diagnosis	5 y	1 y 9 mo	2 mo	35 mo
Initial symptoms	hepatosplenomegaly	hepatosplenomegaly and right testicular swelling	Coughing, rhinorrhea, and feeding difficulty	Progressive dyspnea, systolic murmur, and hepatomegaly
Laboratory findings/ imagings	8% of 1.4×10^9/L leukocytes in peripheral blood, 98% lymphoblasts in bone marrow: positive for TdT, HLA-DR, CD34, CD13, CD33, CD19, CD10, CD22, and CD79	100% of 8.3×10^{10}/L leukocytes in peripheral blood, 98% lymphoblasts in bone marrow: positive for TdT, HLA-DR, CD19, CD10, CD22, and CD79	Right lung pneumonia with pleurisy; cytologic examination of pleural fluid showed T-cell lymphoblasts: positive for CD2, CD3, CD5, and CD7	Intracardiac mass in the right atrium, extending into the inferior vena cava, to a level close to the renal veins; 5.2×6.4 cm intrahepatic mass infiltrating the posterior branch of the right portal vein and extending into the right hepatic lobe
Treatment	Vincristine, dexamethasone and *E. coli* asparginase for induction therapy	Vincristine, predonsolone, *E. coli* asparginase, and doxorubicin for induction therapy	Vincristine, predonisolone, tetrahydropyranyl adriamycin, cyclophosphamide, and *E. coli* asparaginase	Surgical dissection of intracardiac mass revealed hepatoblastoma, cisplatin, vincristine, and 5-flurouracil as chemotherapy
Outcome	Healthy at 15 y of age	Healthy as of age 9 y 3 mo	Healthy as of age 12 y 4 mo	Died at 35 mo

ALL indicates acute lymphoblastic leukemia; ASD, atrial septal defect; CFC, cardiofaciocutaneous syndrome; E. coli, Escherichia coli; HLA_DR, human leucocyte antigen-DR; PS, pulmonic stenosis; TdT, terminal deoxynucleotidyl transferase.

TABLE 2. *BRAF* Mutations Identified in Hematologic Malignancies

Nucleotide Change	Amino Acid Change	Malignant Tumor	References
c. 1402 G > C	p.G468R	Diffuse large B-cell lymphoma	22
c. 1403 G > C	p.G468A	Diffuse large B-cell lymphoma	22
c. 1403 G > C	p.G468A	Diffuse large B-cell lymphoma	22
c. 1403 G > C	p.G468A	B-cell ALL	23
c. 1403 G > C	p.G468A	B-cell ALL	23
c. 1403 G > C	p.G468A	Bisphenotypic acute leukemia	23
c. 1403 G > C	p.G468A	AML	23
c. 1768G > A	p.V590I	Pre-B ALL	24
c. 1778A > G	p.D593G	Diffuse large B-cell lymphoma	22
c. 1786G > A	p.G596S	T-ALL	24
c. 1790T > A	p.L597Q	Pre-B ALL	24
c. 1790T > A	p.L597Q	Pre-B ALL	24
c. 1790T > A	p.L597Q	Pre-B ALL	24
—	p.V600E	U266 myeloma cells	25, 26
c.1796T > A	p.V600E	t-AML(M5)	27
c.1796T > A	p.V600E	t-AML(M5)	27
c.1796T > A	p.V600E	t-AML(M5)	27
c.1796T > A	p.V600E	T-ALL	24

ALL indicates acute lymphoblastic leukemia; t-AML, therapy-related acute myeloid leukemia; T-ALL, T-cell ALL.

B-cell lymphoma (2 cases with G468A, 1 with G468R, and 1 with D593G) and 4 cases with leukemia (G468A) (Table 2).[23] Gustafsson et al[24] investigated exons 11 and 15 of *BRAF* in 29 cases with pre-B ALL (25 cases), T-cell ALL (3 cases), and undifferentiated ALL (1 case) and identified *BRAF* mutations in 6 cases (21%). Christiansen et al[27] identified 3 BRAF mutations in 3 of 51 therapy-related acute myeloid leukemia patients, but not in therapy-related myelodysplasia. In contrast, Davidsson et al[28] did not identify any BRAF mutations in 92 B-cell precursor ALL and 17 T-cell ALL. In other studies, no *BRAF* mutations were identified in 86 cases with childhood ALL,[29] in 104 cases with acute myeloid leukemia, [30] and in 65 cases with juvenile myelomonocytic leukemia.[31] Recently, it has been postulated that 2 general types of gene mutation cooperate to produce leukemogenesis.[32] Class I mutations are those with receptor tyrosine kinases or genes downstream in the RAS/RAF/MEK/extracellular signal-regulated kinase pathway, which result in a proliferative or survival advantage. Class II mutations impair hematologic differentiation. BRAF is a member of the RAF serine/threonine family and transmits the RAS signal to downstream MEK/ERK. Somatic mutations in *BRAF* have been identified in approximately 7% of tumors, including malignant melanoma, pancreatic tumors, and lung cancer.[2] BRAF mutations are involved in Class I mutation and possibly contribute to leukemogenesis.

ACKNOWLEDGMENTS

The authors thank the patient and his family who participated in this study. The patient's parents have given permission for the use of the figure in the article. They also thank Dr Raoul CM Hennekam for informing us about the outcome of his patient.

REFERENCES

1. Reynolds JF, Neri G, Herrmann JP, et al. New multiple congenital anomalies/mental retardation syndrome with cardiofacio-cutaneous involvement–the CFC syndrome. *Am J Med Genet*. 1986;25:413–427.
2. Niihori T, Aoki Y, Narumi Y, et al. Germline KRAS and BRAF mutations in cardio-facio-cutaneous syndrome. *Nat Genet*. 2006;38:294–296.
3. Wieczorek D, Majewski F, Gillessen-Kaesbach G. Cardio-facio-cutaneous (CFC) syndrome—a distinct entity? Report of three patients demonstrating the diagnostic difficulties in delineation of CFC syndrome. *Clin Genet*. 1997;52:37–46.
4. Narumi Y, Aoki Y, Niihori T, et al. Molecular and clinical characterization of cardio-facio-cutaneous (CFC) syndrome: overlapping clinical manifestations with Costello syndrome. *Am J Med Genet A*. 2007;143A:799–807.
5. Aoki Y, Niihori T, Kawame H, et al. Germline mutations in HRAS proto-oncogene cause Costello syndrome. *Nat Genet*. 2005;37:1038–1040.
6. Tartaglia M, Pennacchio LA, Zhao C, et al. Gain-of-function SOS1 mutations cause a distinctive form of Noonan syndrome. *Nat Genet*. 2007;39:75–79.
7. Tartaglia M, Mehler EL, Goldberg R, et al. Mutations in PTPN11, encoding the protein tyrosine phosphatase SHP-2, cause Noonan syndrome. *Nat Genet*. 2001;29:465–468.
8. Roberts AE, Araki T, Swanson KD, et al. Germline gain-of-function mutations in SOS1 cause Noonan syndrome. *Nat Genet*. 2007;39:70–74.
9. Razzaque MA, Nishizawa T, Komoike Y, et al. Germline gain-of-function mutations in RAF1 cause Noonan syndrome. *Nat Genet*. 2007;39:1013–1017.
10. Pandit B, Sarkozy A, Pennacchio LA, et al. Gain-of-function RAF1 mutations cause Noonan and LEOPARD syndromes with hypertrophic cardiomyopathy. *Nat Genet*. 2007;39:1007–1012.
11. Schubbert S, Zenker M, Rowe SL, et al. Germline KRAS mutations cause Noonan syndrome. *Nat Genet*. 2006;38:331–336.
12. Cirstea IC, Kutsche K, Dvorsky R, et al. A restricted spectrum of NRAS mutations causes Noonan syndrome. *Nat Genet*. 2010;42:27–29.
13. Rodriguez-Viciana P, Tetsu O, Tidyman WE, et al. Germline mutations in genes within the MAPK pathway cause cardio-facio-cutaneous syndrome. *Science*. 2006;311:1287–1290.
14. Bentires-Alj M, Kontaridis MI, Neel BG. Stops along the RAS pathway in human genetic disease. *Nat Med*. 2006;12:283–285.
15. Aoki Y, Niihori T, Narumi Y, et al. The RAS/MAPK syndromes: novel roles of the RAS pathway in human genetic disorders. *Hum Mutat*. 2008;29:992–1006.
16. Gripp KW, Scott CI Jr, Nicholson L, et al. Five additional Costello syndrome patients with rhabdomyosarcoma: proposal for a tumor screening protocol. *Am J Med Genet*. 2002;108:80–87.
17. van Den Berg H, Hennekam RC. Acute lymphoblastic leukaemia in a patient with cardiofaciocutaneous syndrome. *J Med Genet*. 1999;36:799–800.
18. Makita Y, Narumi Y, Yoshida M, et al. Leukemia in Cardio-facio-cutaneous (CFC) syndrome: a patient with a germline mutation in BRAF proto-oncogene. *J Pediatr Hematol Oncol*. 2007;29:287–290.
19. Al-Rahawan MM, Chute DJ, Sol-Church K, et al. Hepatoblastoma and heart transplantation in a patient with cardio-facio-cutaneous syndrome. *Am J Med Genet A*. 2007;143A:1481–1488.
20. Smock KJ, Nelson M, Tripp SR, et al. Characterization of childhood precursor T-lymphoblastic lymphoma by immunophenotyping and fluorescent in situ hybridization: a report from the Children's Oncology Group. *Pediatr Blood Cancer*. 2008;51:489–494.
21. Mann G, Attarbaschi A, Burkhardt B, et al. Clinical characteristics and treatment outcome of infants with non-Hodgkin lymphoma. *Br J Haematol*. 2007;139:443–449.

22. Lee JW, Yoo NJ, Soung YH, et al. BRAF mutations in non-Hodgkin's lymphoma. *Br J Cancer*. 2003;89:1958–1960.
23. Lee JW, Soung YH, Park WS, et al. BRAF mutations in acute leukemias. *Leukemia*. 2004;18:170–172.
24. Gustafsson B, Angelini S, Sander B, et al. Mutations in the BRAF and N-ras genes in childhood acute lymphoblastic leukaemia. *Leukemia*. 2005;19:310–312.
25. Velangi M, Matheson E, Taylor P, et al. BRAF gene is not mutated in mismatch repair-proficient or -deficient plasma cell dyscrasias. *Leukemia*. 2004;18:658–659.
26. Ng MH, Lau KM, Wong WS, et al. Alterations of RAS signalling in Chinese multiple myeloma patients: absent BRAF and rare RAS mutations, but frequent inactivation of RAS SF1A by transcriptional silencing or expression of a non-functional variant transcript. *Br J Haematol*. 2003;123:637–645.
27. Christiansen DH, Andersen MK, Desta F, et al. Mutations of genes in the receptor tyrosine kinase (RTK)/RAS-BRAF signal transduction pathway in therapy-related myelodysplasia and acute myeloid leukemia. *Leukemia*. 2005;19:2232–2240.
28. Davidsson J, Lilljebjorn H, Panagopoulos I, et al. BRAF mutations are very rare in B- and T-cell pediatric acute lymphoblastic leukemias. *Leukemia*. 2008;22:1619–1621.
29. Case M, Matheson E, Minto L, et al. Mutation of genes affecting the RAS pathway is common in childhood acute lymphoblastic leukemia. *Cancer Res*. 2008;68:6803–6809.
30. Smith ML, Snaddon J, Neat M, et al. Mutation of BRAF is uncommon in AML FAB type M1 and M2. *Leukemia*. 2003; 17:274–275.
31. de Vries AC, Stam RW, Kratz CP, et al. Mutation analysis of the BRAF oncogene in juvenile myelomonocytic leukemia. *Haematologica*. 2007;92:1574–1575.
32. Komeno Y, Kitaura J, Kitamura T. Molecular bases of myelodysplastic syndromes: lessons from animal models. *J Cell Physiol*. 2009;219:529–534.

Journal of Human Genetics (2010), 1–9

www.nature.com/jhg

ORIGINAL ARTICLE

Mutation analysis of the *SHOC2* gene in Noonan-like syndrome and in hematologic malignancies

Shoko Komatsuzaki[1], Yoko Aoki[1], Tetsuya Niihori[1], Nobuhiko Okamoto[2], Raoul CM Hennekam[3,4], Saskia Hopman[5], Hirofumi Ohashi[6], Seiji Mizuno[7], Yoriko Watanabe[8], Hotaka Kamasaki[9], Ikuko Kondo[10], Nobuko Moriyama[11], Kenji Kurosawa[12], Hiroshi Kawame[13], Ryuhei Okuyama[14], Masue Imaizumi[15], Takeshi Rikiishi[16], Shigeru Tsuchiya[16], Shigeo Kure[1,16] and Yoichi Matsubara[1]

Noonan syndrome is an autosomal dominant disease characterized by dysmorphic features, webbed neck, cardiac anomalies, short stature and cryptorchidism. It shows phenotypic overlap with Costello syndrome and cardio-facio-cutaneous (CFC) syndrome. Noonan syndrome and related disorders are caused by germline mutations in genes encoding molecules in the RAS/MAPK pathway. Recently, a gain-of-function mutation in *SHOC2*, p.S2G, has been identified as causative for a type of Noonan-like syndrome characterized by the presence of loose anagen hair. In order to understand the contribution of *SHOC2* mutations to the clinical manifestations of Noonan syndrome and related disorders, we analyzed *SHOC2* in 92 patients with Noonan syndrome and related disorders who did not exhibit *PTPN11*, *KRAS*, *HRAS*, *BRAF*, *MAP2K1/2*, *SOS1* or *RAF1* mutations. We found the previously identified p.S2G mutation in eight of our patients. We developed a rapid detection system to identify the p.S2G mutation using melting curve analysis, which will be a useful tool to screen for the apparently common mutation. All the patients with the p.S2G mutation showed short stature, sparse hair and atopic skin. Six of the mutation-positive patients showed severe mental retardation and easily pluckable hair, and one showed leukocytosis. No *SHOC2* mutations were identified in leukemia cells from 82 leukemia patients. These results suggest that clinical manifestations in *SHOC2* mutation-positive patients partially overlap with those in patients with typical Noonan or CFC syndrome and show that easily pluckable/loose anagen hair is distinctive in *SHOC2* mutation-positive patients.
Journal of Human Genetics advance online publication, 30 September 2010; doi:10.1038/jhg.2010.116

Keywords: cardio-facio-cutaneous syndrome; costello syndrome; hematologic malignancy; loose anagen hair; melting curve analysis; noonan syndrome

INTRODUCTION

Noonan syndrome (MIM 163950) is an autosomal dominant disorder characterized by short stature, webbed or short neck, characteristic features (hypertelorism, low-set ears and ptosis), pulmonary valve stenosis and hypertrophic cardiomyopathy.[1,2] Noonan syndrome is a heterogeneous disease and overlaps phenotypically with Costello syndrome (MIM 218040) and cardio-facio-cutaneous (CFC) syndrome (MIM 115150). Costello syndrome is characterized by mental retardation, distinctive facial features, neonatal feeding difficulties, curly hair, loose skin, and hypertrophic cardiomyopathy and carries an increased risk of malignancy.[3] CFC syndrome, on the other hand, is characterized by mental retardation, ectodermal abnormalities (sparse hair, hyperkeratotic skin and ichthyosis), distinctive facial features (high forehead, bitemporal constriction, hypoplastic supraorbital ridges, downslanting palpebral fissures and depressed nasal bridge) and congenital heart defects (pulmonic stenosis, atrial septal defect and hypertrophic cardiomyopathy).[4]

Recent studies have shown that all three of these disorders result from dysregulation of the RAS/MAPK cascade. It has been suggested that these syndromes be comprehensively termed the RAS/MAPK syndromes[5] or the neuro-cardio-facial-cutaneous syndrome.[6] Germline mutations in *PTPN11*, *KRAS*, *SOS1* and *RAF1* have been

[1]Department of Medical Genetics, Tohoku University School of Medicine, Sendai, Japan; [2]Department of Medical Genetics, Osaka Medical Center and Research Institute for Maternal and Child Health, Izumi, Osaka, Japan; [3]Clinical and Molecular Genetics Unit, Institute of Child Health, Great Ormond Street Hospital for Children, University College London, London, UK; [4]Department of Pediatrics, Academic Medical Center, University of Amsterdam, Amsterdam, The Netherlands; [5]Department of Pediatric Oncology, Emma Children's Hospital, Academic Medical Center, Amsterdam, The Netherlands; [6]Division of Medical Genetics, Saitama Children's Medical Center, Saitama, Japan; [7]Department of Pediatrics, Central Hospital, Aichi Human Service Center, Aichi, Japan; [8]Department of Pediatrics and Child Health, Kurume University School of Medicine, Kurume, Japan; [9]Department of Pediatrics, Sapporo Medical University, Sapporo, Japan; [10]Division of Pediatrics, Oida Hospital, Kochi, Japan; [11]Department of Pediatrics, Hitachi Ltd, Mito General Hospital, Ibaraki, Japan; [12]Division of Medical Genetics, Kanagawa Children's Medical Center, Yokohama, Japan; [13]Department of Genetic Counseling, Ochanomizu University, Tokyo, Japan; [14]Department of Dermatology, Shinshu University School of Medicine, Matsumoto, Japan; [15]Department of Hematology and Oncology, Miyagi Children's Hospital, Sendai, Japan and [16]Department of Pediatrics, Tohoku University School of Medicine, Sendai, Japan
Correspondence: Dr Y Aoki, Department of Medical Genetics, Tohoku University School of Medicine, 1-1 Seiryo-machi, Sendai, Miyagi 980-8574, Japan.
E-mail: aokiy@med.tohoku.ac.jp
Received 14 June 2010; accepted 15 August 2010

identified in 60–80% of Noonan syndrome patients.[7–12] In patients with Costello syndrome, germline mutations in *HRAS* have been identified,[13] and mutations in *KRAS*, *BRAF* or *MAP2K1/MAP2K2* have been identified in approximately 70% of patients with CFC syndrome.[14,15] However, in approximately 40% of patients with these disorders, specific mutations have not been identified.

SHOC2 is homologous to *soc2*, a gene that was discovered in *Caenorhabditis elegans*. The *soc2* gene encodes leucine-rich repeats[16] and acts as a positive modulator of the RAS/MAPK pathway.[17] Recently, Cordeddu *et al*.[18] reported a gain-of-function missense mutation, c.4A>G (p.S2G), in *SHOC2* in patients with Noonan-like syndrome with loose anagen hair. However, clinical features of patients with a mutation in *SHOC2* remain unknown. In this study, we analyzed 92 patients with Noonan syndrome and related disorders to characterize mutations in the *SHOC2* gene. We also performed expression analysis of *SHOC2* in adult and fetal human tissues and performed sequence analysis of *SHOC2* in 82 leukemia samples.

MATERIALS AND METHODS

DNA samples from patients with Noonan syndrome and related disorders and from leukemia cells

We analyzed 92 patients with Noonan syndrome and related disorders who did not display *PTPN11*, *KRAS*, *HRAS*, *BRAF*, *MAP2K1/2* (*MEK1/2*), *SOS1* or *RAF1* mutations. At the time at which samples were sent, the primary diagnoses of these patients were as follows: 34 Noonan syndrome, 17 Costello syndrome, 21 CFC syndrome, 4 Noonan/CFC, 2 Costello/CFC and 14 others. Control DNA was obtained from 132 healthy Japanese individuals. Control DNA from 105 healthy Caucasian individuals was purchased from Coriell Cell Repositories (Camden, NJ, USA). Eighty-two leukemia DNA samples were collected from leukemia patients (32 acute myeloid leukemia, 41 acute lymphoblastic leukemia, 1 juvenile chronic myelogenous leukemia, 1 Ki-lymphoma, 2 malignant lymphoma, 1 myelodysplastic syndrome, 1 aplastic anemia, 2 transient abnormal myelopoiesis and 1 unknown). Nine additional genomic DNA samples were collected from patients who had developed leukemia and had achieved complete remission (eight acute lymphoblastic leukemia and one aplastic anemia).

This study was approved by the Ethics Committee of Tohoku University School of Medicine. We obtained informed consent from all subjects involved in the study and specific consent for photographs from seven patients.

Analysis of *SHOC2* mutations

Genomic DNA was extracted from patients' peripheral leukocytes. Exons and flanking intron sequences of *SHOC2* were amplified by PCR with primers based on GenBank sequences (Supplementary Table 1, GenBank accession no. NC_000010.10). The M13 reverse or forward sequence was added to the 5′ end of the PCR primers for use as a sequencing primer. PCR was performed in 15 μl of solution containing 67 mM Tris-HCl (pH 8.8), 6.7 mM $MgCl_2$, 17 mM NH_4SO_4, 6.7 μM EDTA, 10 mM β-mercaptoethanol, 1.5 mM dNTPs, 10% (v/v) dimethylsulfoxide (except fragment 7), 1 μM of each primer, 50 ng genomic DNA and 1 unit of Taq DNA polymerase. The reaction consisted of 37 cycles of denaturation at 94 °C for 20 s, annealing at the indicated temperature for 30 s and extension at 72 °C for 30 s. The PCR products of fragment 1a were gel purified; PCR products of the other fragments were purified using MultiScreen PCR plates (Millipore, Billerica, MA, USA). The purified PCR products were sequenced on an ABI PRISM 3130 automated DNA sequencer (Applied Biosystems, Foster City, CA, USA).

Development of a mutation detection system using the light cycler

Real-time PCR and melting curve analysis to detect the c.4A>G mutation was developed using the LightCycler system (Roche Diagnostics, Mannheim,

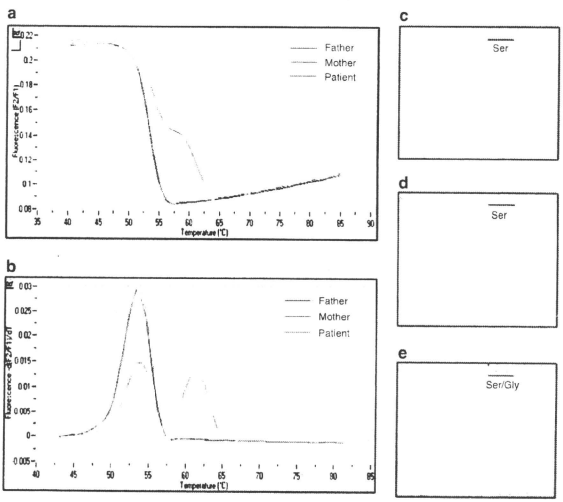

Figure 1 (**a**) PCR followed by melting analysis to detect the c.4A>G mutation. F2 represents the fluorescence emission of the LC Red 640 fluorophore, whereas F1 shows the fluorescence emission of the fluorescein fluorophore. (**b**) Melting curves are automatically converted into melting peaks, which are given as the first negative derivative of the fluorescence (F) versus temperature (T) (-dF/dT) (*y* axis) versus temperature (temp)(*x* axis). The homozygous wild-type allele (parents of NS128) shows a single melting temperature, whereas the heterozygote (NS128) shows two different melting temperatures. (**c**, **d**) Sequencing traces of parents of NS128. (**e**) Sequencing trace of NS128.

Germany). Primer and probe sequences are shown in Supplementary Table 2. The acceptor probe, which matches the mutant allele sequence, was labeled at its 3′ end with fluorescein isothiocyanate. The donor probe was labeled at its 5′ end with LC Red640 and phosphorylated at its 3′ end to prevent probe elongation by the Taq polymerase. Probes were designed by Nihon Gene Research Laboratories (Sendai, Japan). Amplification was performed in a final volume of 20 μl in glass capillaries containing 10 ng of sample DNA, 2 μl of 10× LightCycler-FastStart DNA Master HybProbe (Roche Diagnostics), 12 nM $MgCl_2$, 0.3 μM of each forward and reverse primer and 0.2 μM of each acceptor and donor hybridization probe. PCR was performed under the following conditions: initial denaturation at 95 °C for 10 min, 40 cycles of 95 °C for 10 s, 60 °C for 15 s and 72 °C for 7 s with a ramping time of 20 °C s^{-1}. After amplification, melting curve analysis was performed under the following conditions: 95 °C with 0-s hold, cooling to 40 °C for 30 s and slowly heating the sample to 85 °C with a ramp rate of 0.4 °C s^{-1}.

Real-time quantitative PCR

MTC Multiple Tissue cDNA panels Human 1, 2, Human Fetal, Human Immune and Human Cell Line (Clontech, Palo Alto, CA, USA) were used to evaluate the relative expression of *SHOC2* in various tissues. Separation of mononuclear and polymorphonuclear (PMN) leukocytes from whole blood was performed using Polymorphoprep (Nycomed, Oslo, Norway); total RNA was prepared with the RNeasy Mini Kit (Qiagen, Hilden, Germany). One hundred ng of total RNA was used to synthesize complementary DNA (cDNA) using the High Capacity cDNA Reverse Transcription kit (ABI). Primers for real-time PCR were designed using software provided by Roche (https://www.roche-applied-science.com) (Supplementary Table 3). Universal ProbeLibrary #42 and #60 (Roche) were used for *SHOC2* and *GAPDH*, respectively. PCR was performed in 20 μl of solution containing 10 μl FastStart Universal Probe Master (Rox) (Roche), 18 pmol of each primer, 5 μl cDNA and 0.25 μM universal HybProbe. The reaction conditions were 50 °C for 2 min and 95 °C for 10 min, followed by 40 cycles of 95 °C for 15 s and 60 °C for 11 min. The real-time PCR program was run by the 7500 Real-Time PCR system (ABI). Diluted control cDNA (1:1, 1:10, 1:100, 1:1000 and 1:10 000) from Multiple Tissue cDNA panels (Clontech) was amplified with each reaction in order to generate a standard curve and calculate relative gene expression of *SHOC2*.

RESULTS

Mutation analysis in patients and development of a rapid mutation detection system

Sequence analysis of all coding regions of *SHOC2* in 92 patients revealed a c.4A>G mutation (p.S2G) in exon1 of *SHOC2* in eight unrelated patients. Parental samples were available in three families; the mutation was not identified in parents, suggesting that the mutation occurred *de novo*.

Our results and the previous report identified a c.4A>G mutation in patients with Noonan-like syndrome. To further characterize the occurrence of this mutation, we developed a rapid mutation detection system using a Lightcycler. Two probes were generated for melting curve analysis, and melting curve analysis was performed after PCR. The PCR products from a patient heterozygous for the c.4A>G mutation differed from those obtained from the patient's parents as well as from those obtained from control subjects (Figures 1a and b). The PCR products were verified by sequencing (Figures 1c–e).

Clinical manifestations of patients with the *SHOC2* mutation

The clinical manifestations of eight patients with the *SHOC2* mutation are shown in Table 1; photographs of five of these patients are shown in Figure 2. The ages of the patients ranged from 4 to 25 years. The primary diagnoses for these patients were Costello, Noonan or CFC syndrome. Three had perinatal abnormalities, including tachypnea, hydramnios, pulmonary hemorrhage and intracranial hemorrhage.

Table 1 Clinical manifestations in *SHOC2* mutation-positive patients

Patient ID	*NS34*	*NS93*	*NS97*	*NS121*	*NS128*	*NS180*	*NS220*	*NS232*
SHOC2 mutation	p.S2G	p.S2G	p.S2G	p.S2G	p.S2G	p.S2G	p.S2G	p.S2G
Genotype of father/mother	WT/WT	ND	ND	ND	WT/WT	ND	ND	WT/WT
Gender	M	F	F	M	F	M	F	M
Age (years)	13.8	21	10	5.7	8	9	4	25
Country	Japan	The Netherlands	Japan	Japan	Japan	Japan	Japan	Japan
Primary diagnosis	NS/CFC	CFC	CFC	CFC	CFC	NS	CS	CS
Perinatal abnormality	+	ND	–	–	–	+	+	–
Polyhydramnios	–	ND	–	–	–	+	–	–
Birth weight	3118 g	3360 g	3068 g	2865 g	2308 g	3258 g	3160 g	3090 g
Others	Tachypnea					Pulmonary hemorrhage	Intracranial hemorrhage	
Growth and development								
Failure to thrive	+	+	+	+	+	+	+	+
Mental retardation	+ WISC III at 9 years 3 months VIQ 81, PIQ 87, FIQ 82	–	+ (DQ44)	+ (DQ48)	+ (DQ 66)	+ WISC III at 9 years 4 months VIQ 61, PIQ <40 FIQ 45	+ (DQ53)	+ (IQ65)
Hyperactivity	–	–	+	–	–	–	–	– (irritability in infancy)
Delayed independent walking (age)	+ (3.6 years)	–	+ (1.8 years)	+ (2.8 years)	+ (4 years)	+ (5 years)	+ (4 years)	+ (3.6 years)
Craniofacial characteristics								
Relative macrocephaly	+	+	+	+	+	+	+	+
Hypertelorism	+	–	–	–	–	+	–	+

Table 1 Continued

Patient ID	*NS34*	*NS93*	*NS97*	*NS121*	*NS128*	*NS180*	*NS220*	*NS232*
Downslanting palpebral fissures	+	+	+	–	–	+	–	–
Ptosis	–	+	–	+	–	–	–	–
Epicanthal folds	–	–	+	+	–	+	+	±
Low-set ears	+	+	+	+	+	+	+	+
Highly arched palate	+	+	–	+	+	–	+	+
Prominent forehead	ND	–	+	+	ND	ND	+	ND
Broad forehead	+	+	+	+	+	+	+	ND
Skeletal characteristics								
Short stature	−3.4 s.d. at 13 years	−3 s.d. at 21 years	−4 s.d. at 6 years	−3 s.d. at 1 year 9 months	−5 s.d. at 8 years	−6 s.d. at 9 years	−4.5 s.d. at 3 years 3 months	−2 s.d. at 23 years
Short neck	+	+	–	+	+	+	–	+
Webbing of neck	+	+	–	–	–	–	–	±
Cubitus valgus	+	+	–	–	–	–	–	–
Pectus anomalies	ND	–	+	+	–	+	–	–
Cardiac defects								
Hypertrophic cardiomyopathy	–	–	+	–	+	+	±	–
Atrial septal defect	–	–	+	–	–	–	+	+
Ventricular septal defect	–	–	–	–	–	–	–	+
Pulmonary stenosis	+	–	+	–	+	–	+	–
Mitral valve anomaly	+	–	–	–	–	–	–	+
Others	Pulmonary regurgitation	Arrhythmia						Hypoplasia of papillary muscle
Hair anomalies								
Curly hair	–	–	+	+	+	+	+	+
Sparse hair	+	+	+	+	+	+	+	+
Easily pluckable hair	+	+	+	+	+	ND	+	+
Skin anomalies								
Dark skin	+	+	+	+	+	+	+	+
Hyperkeratosis	ND	+	+	+	+	–	–	+
Hyperelastic skin	+	–	+	+	+	–	–	+
Café-au-lait spots	+	–	–	–	–	–	–	–
Lentigines	+	–	–	–	–	+	–	–
Atopic skin/eczema	+	+	+	+	+	+	+	+
Others					Deep palmar/ planter creases			Facial erythema, nummular eczema
Genital abnormalities	+ (Cryptorchidism)	–	–	–	–	+(Cryptorchidism)	–	–
Blood test abnormality								
Coagulation defect (normal range)	+[a]	ND	–	+[b]	ND	+[c]	–	–
Number of white blood cells/(μl) (normal range for patient's age)	7200 (5000–10 000)	8400 (5000–10 000)	16 000 (4500–13 500)	5300 (6000–15 000)	10 900 (4500–13 500)	9900 (4500–13 500)	10 300 (6000–15 000)	9900 (5000–10 000)
Polymorph nuclear cell (%) (mean for each patient's age)	60 (55)	ND	79 (55)	ND	50 (55)	72 (55)	53 (45)	77 (55)
IgE (U ml^{-1})	ND	ND	2300	94	ND	1800	ND	820
Hypernasal/hoarse voice	ND	–	+	+	–	ND	+	+
Miscellaneous	GH deficiency	Delayed puberty, EEG abnormalities, easy bruising	GH deficiency	GH deficiency	Adenoid hypertrophy, GH deficiency		Dilatation of cerebral ventricles, epilepsy	Congenital hydro-nephrosis, frostbite in winter

Abbreviations: APTT, activated partial thrombin time; AT, antithrombin; BT, bleeding time; CFC, cardio-facio-cutaneous; CS, Costello syndrome; DQ, developmental quotient; EEG, electroencephalogram; FIQ, Full Scale intelligence quotient; GH, growth hormone; ND, not described; NS, Noonan syndrome; PIQ, Performance intelligence quotient; PT, prothrombin time; VIQ, verbal intelligence quotient; WISC, Wechsler Intelligence Scale for Children; WT, wild type.
[a]The test was performed when bloody stool was observed at 7 years of age. BT 180 sec (2.5–13), PT 11.5 sec (10.1–12.0) APTT 62.5 sec (26–37), Factor VIII 53% (52–120). Parenthesis represents normal range for the patient's age.
[b]APTT 54 sec (26–37), Factor IX 22% (47–104), Factor XII 34% (64–129), Factor XIII 51 (72–143). Parenthesis represents normal range for the patient's age.
[c]APTT 57 sec (26–37). Parenthesis represents normal range for the patient's age.

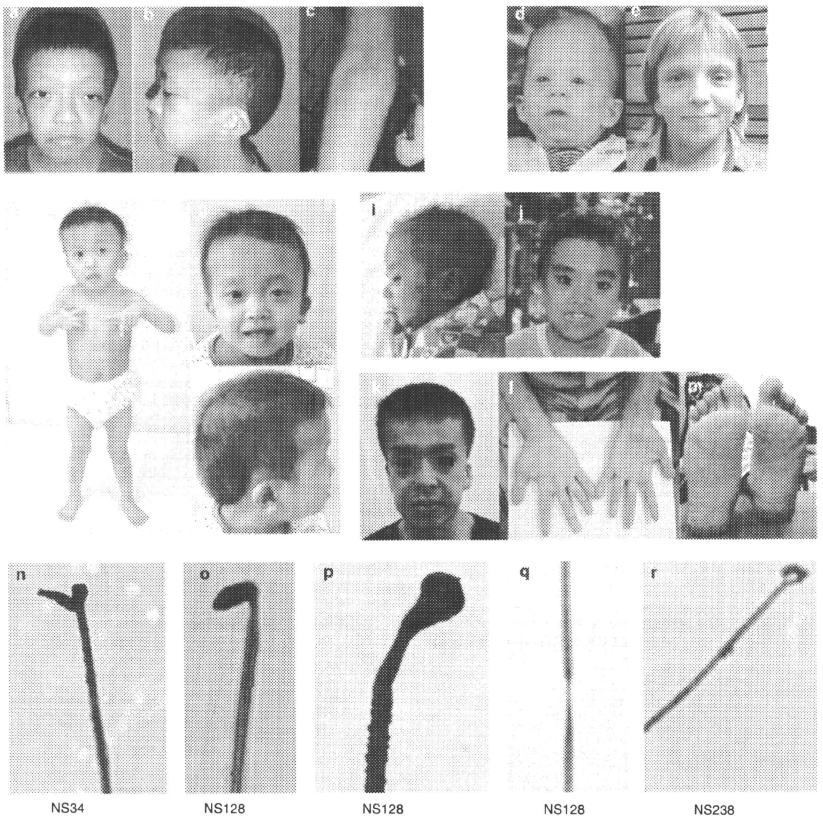

Figure 2 (**a**, **b**) Facial appearance of NS34 at the age of 13 years. (**c**) Dry and atopic skin seen in NS34. (**d**, **e**) NS93. (**f–h**) NS97. (**i**, **j**) NS128. (**k–m**) NS232 at the age of 25 years. (**l**, **m**) Palms and soles of NS232 showing fine wrinkling. Light micrographs of hairs from patients NS34 (**n**), NS128 (**o–q**) and NS238 (**r**). The hair bulb is distorted at an acute angle to the hair shaft, a characteristic described as 'mousetail deformity.' The hair shaft is twisted and longitudinally grooved.

All showed short stature $\geqslant -2$ s.d.) despite normal growth during the fetal period. Mild-to-moderate mental retardation was observed in seven patients. It is of note that delayed independent walking was observed in seven patients. The facial appearances of these patients changed with age. Features frequently observed were relative macrocephaly (8/8 patients), low-set ears (8/8), highly arched palate (6/8) and broad forehead (7/7). Cardiac abnormalities included hypertrophic cardiomyopathy in four patients, atrial septal defect in three patients, pulmonic stenosis in four patients and mitral valve anomaly in two patients. Atopic skin and eczema were observed in all eight patients (Figure 2c), and serum immunoglobulin E level was elevated in three patients. Seven patients had sparse and easily pluckable hair. The hair bulb was bent at an acute angle to the hair shaft, which was irregular and twisted (Figures 2n–r). Four patients had hyponasal/hoarse voice as previously described[18] and three patients showed coagulation defects with prolonged activated partial thrombin time.

The clinical history of two adult patients, NS232 and NS93, differed from those of patients typical for Noonan syndrome. NS232 was a 25-year-old patient, the first son of unrelated healthy parents. Delivery

at 40 weeks was uncomplicated, and birth weight was 3090 g. At 1 month of age, this patient was diagnosed as having an atrioventricular septal defect; the defect spontaneously closed at 5 months of age. During the infantile period, this patient showed irritability and mental/motor delay: head control was achieved at 1 year and 10 months, sitting at 2 years and 4 months and walking at 3 years and 6 months. At his infantile period, this patient was suspected to have Noonan syndrome or Costello syndrome. Pyelostomy for congenital hydronephrosis was performed at the age of 10 months. At 23 years of age, mitral valve replacement was performed because of mitral valve prolapse (III–IV). The dissected mitral valve showed myxomatous change. At 25 years, this patient shows mild mental retardation and displays a gentle personality. Other characteristics include hypertelorism, a highly arched palate and posteriorly rotated ears. During infancy, his hair was pluckable, but the hair abnormality is now subtle. He possesses variable skin abnormalities including fine wrinkles on the palm and soles as well as erythematous rash on the face and eczematous skin changes on the trunks and extremities together with xerotic skin, which are reminiscent of atopic dermatitis (Figures 2k–m). Another adult patient, NS93, has been diagnosed as having CFC syndrome at 1 year of age (Figure 2d). Subsequently her normal motor development and her cognitive development that fell within normal ranges (but was lower than other family members) shed doubt about this diagnosis. She had a delayed pubertal development. She has quite a marked tendency to have bleeding episodes after surgery and to bruise easily.

Leukocytosis in the absence of obvious infection was observed in one of the patients (NS97). The white blood cell count of this patient ranged from 16 000 to 23 000/μl at 5 years of age. The number of leukocytes of the other patients was within the normal range, but close to the upper limit of the normal range.

Expression of *SHOC2* mRNA

A previous study using northern blot analysis showed that *SHOC2* mRNA is present in most tissues, including brain, heart, kidney and pancreas.[16] Because leukocytosis was observed in a patient with the p.S2G mutation, we examined the relative expression of *SHOC2* in various tissues including blood leukocytes and lymphocytes. In the adult human cDNA panel, the highest expression was observed in testis; relatively high expression was also observed in several immune tissues (spleen, bone marrow, tonsil and lymph node) (Figures 3a and b). The expression of *SHOC2* was six times higher in PMN than mononuclear (Figure 3c). Among fetal tissues, brain showed the highest expression (Figure 3d). No increase in *SHOC2* expression was observed in cultured tumor cells (Figure 3e).

SHOC2 mutation analysis in samples from patients with hematologic malignancies

Patients with Noonan-related disorders develop various solid tumors and hematologic malignancies.[5] Approximately 10% of patients with Costello syndrome develop rhabdomyosarcoma, ganglioneuroblastoma or bladder carcinoma. Patients with Noonan syndrome occasionally develop juvenile myelomonocytic leukemia or leukemia.[2] Recently, the occurrence of ALL or non-Hodgkin's lymphoma has been reported in three patients with CFC syndrome.[5,19,20] The presence of leukocytosis in mutation-positive patients and the high expression of *SHOC2* mRNA in PMN led us to look for possible *SHOC2* mutations in patients with hematologic malignancies. However, no such mutations were identified in any of the leukemia samples or in the genomic DNA samples from patients who had been treated for leukemia.

DISCUSSION

In this study, we identified the c.4A>G (p.S2G) mutation in *SHOC2* in 8 of 92 (9%) otherwise mutation-negative patients with Noonan syndrome or related disorders. The mutation detection rate was higher than that reported in a previous study, in which 21 of 410 (5%) such patients were found to carry this mutation. By parental examination, the current and previous studies confirmed *de novo* mutation in 3 and 12 families, respectively. Quantitative PCR analysis demonstrated that

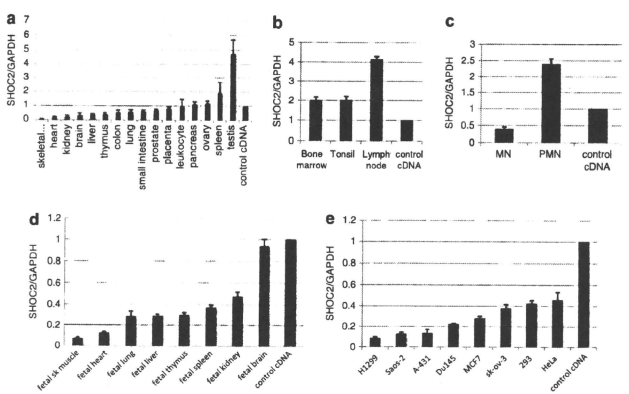

Figure 3 Relative expression of *SHOC2*. Expression levels of *SHOC2* mRNA in various adult human tissues (**a**), adult immune tissues (**b**), human leukocytes (**c**), human fetal tissues (**d**) and human tumor cell lines (**e**) were evaluated by quantitative PCR using *GAPDH* mRNA as the control. Results are expressed as the means and s.d.s of mean values from triplicate samples. Control DNA supplied with Clontech cDNA panels was used as a control.

Table 2 Summary of clinical manifestations in patients with CFC syndrome, Noonan-like syndrome and Noonan syndrome

	CFC syndrome (%)	*Noonan-like syndrome (%)*	*Noonan syndrome (%)*
References	20,21[a]	Cordeddu *et al*,[18] and this study	22
Gene mutations	*KRAS*, *BRAF* and *MAP2K1/2*	*SHOC2*	*PTPN11*, *KRAS*, *SOS1* and *RAF1*
Total patients	63	33	315
Perinatal abnormality			
Polyhydramnios	23/30 (77)	1/7 (14)	21/50 (42)
Fetal macrosomia	ND	ND	20/46 (43)
Growth and development			
Failure to thrive	24/36 (67)	8/8 (100)	51/74 (69)
Mental retardation	25/25 (100)	27/32 (84)	124/293 (42)
Craniofacial characteristics			
Relative macrocephaly	40/58 (69)	31/33 (94)	50/70 (71)
Hypertelorism	17/25 (68)	26/33 (79)	66/82 (80)
Downslanting palpebral fissures fissures fissures	20/25 (80)	4/8 (50)	77/99 (78)
Ptosis	12/25 (48)	24/33 (73)	75/105 (71)
Epicanthal folds	13/25 (52)	5/8 (63)	41/72 (57)
Low-set ears	20/25 (80)	30/33 (91)	115/132 (87)
Skeletal characteristics			
Short stature	46/63 (73)[b]	32/32 (100)	172/297 (58)
Short neck	22/25 (88)	23/33(70)	76/107 (71)
Webbing of neck	6/25(24)	20/33 (61)	84/188 (45)
Cardiac defects			
Hypertrophic cardiomyopathy	24/58 (41)	9/33 (27)	57/277 (21)
Atrial septal defect	11/57 (19)	11/33 (33)	20/69 (29)
Ventricular septal defect	7/57 (12)	3/33(9)	7/70 (10)
Septal defect total	18/57 (32)	14/33 (42)	85/313 (27)
Pulmonic stenosis	23/58 (40)	13/33 (39)	196/312 (63)
Patent ductus arteriosus	ND	0/33 (0)	3/38 (8)
Mitral valve anomaly	10/63 (16)[a]	10/32 (31)	16/67 (24)
Arrhythmia	4/63 (6)	1/33 (3)	14/25 (56)
Skeletal/extremity deformity			
Cubitus valgus	6/25 (24)[a]	2/8 (25)	26/100 (26)
Pectus deformity	27/54 (50)	23/32 (72)	184/287 (64)
Skin/hair anomaly			
Curly hair	58/63 (92)	6/8 (75)	30/75 (40)
Sparse hair	56/63 (89)	33/33 (100)	ND
Loose anagen hair/easily pluckable hair	ND	19/19(100)	ND
Hyperelastic skin	7/25 (28)[a]	5/8 (63)	16/51 (31)
Café-au-lait spots	13/58 (22)[a]	1/8 (13)	5/49 (10)
Lentigines	ND	2/8 (25)	3/49 (6)
Nevus	37/62 (60)[a]	ND	12/46 (26)
Genitalia			
Cryptorchidism	11/41(27)[a]	8/25 (32)	114/211 (54)
Blood test abnormality			
Coagulation defects	1[c]	9/29 (31)	65/180 (36)

Abbreviations: CFC, cardio-facio-cutaneous; ND, not described.
[a]Includes our unpublished data.
[b]Includes short stature (height below the 3rd centile).
[c]A patient with von Willebrand disease was reported.